AD-A181 665 SHEAROGRAPHIC IMAGING SYSTEM(U) UNIVERSITY COLL OF NORTH WALES BANGOR SCHOOL OF ELECTRONIC ENGINEERING SCIENCE D K DAS-GUPTA 01 JUN 87 RVK-50 1/1

UNCLASSIFIED DAJA45-84-C-0042 F/G 20/6 NL

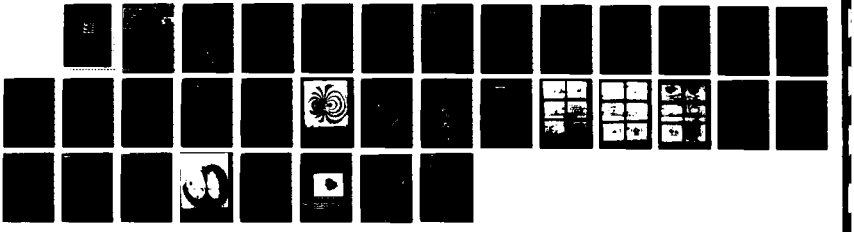

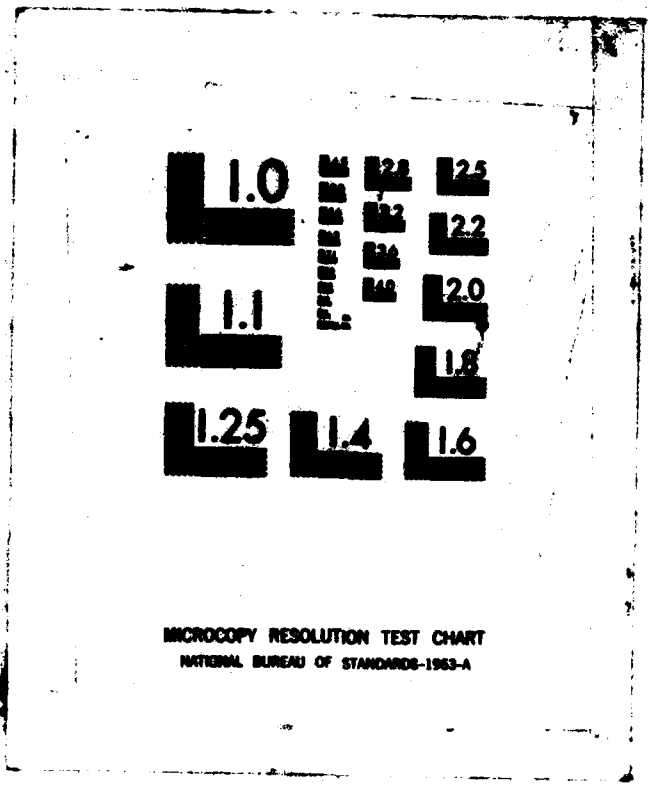
1.0
1.1
1.25
1.4
1.6
2.0
2.2
2.5
MICROCOPY RESOLUTION TEST CHART
NATIONAL BUREAU OF STANDARDS-1963-A

6a. NAME OF PERFORMING ORGANIZATION	6b. OFFICE SYMBOL (If applicable)	7a. NAME OF MONITORING ORGANIZATION
University College of North Wales	UCNW/SEES	USAR DSG-UK

6c. ADDRESS (City, State, and ZIP Code)	7b. ADDRESS (City, State, and ZIP Code)
School of Electronic Engineering Science Dean Street, Bangor, Gwynedd, LL57 1UT	"Edison House" 223 Old Marylebone St, London NW1 5TH

8a. NAME OF FUNDING/SPONSORING ORGANIZATION	8b. OFFICE SYMBOL (If applicable)	9. PROCUREMENT INSTRUMENT IDENTIFICATION NUMBER
USAR DSG-UK	—	—

8c. ADDRESS (City, State, and ZIP Code)	10. SOURCE OF FUNDING NUMBERS			
	PROGRAM ELEMENT NO.	PROJECT NO.	TASK NO.	WORK UNIT ACCESSION NO.
"Edison House" 223 Old Marylebone St, London NW1 5TH	—	—	—	—

11. TITLE (Include Security Classification)

Shearographic Imaging System (unclassified)

12. PERSONAL AUTHOR(S) Dr. D.K. Das-Gupta

13a. TYPE OF REPORT	13b. TIME COVERED	14. DATE OF REPORT (Year, Month, Day)	15. PAGE COUNT
Final	FROM 16.10.84 TO 16.12.86	1987, June 1987, June 15	31

16. SUPPLEMENTARY NOTATION

—

17. COSATI CODES			18. SUBJECT TERMS (Continue on reverse if necessary and identify by block number)
FIELD	GROUP	SUB-GROUP	
—	—	—	—

19. ABSTRACT (Continue on reverse if necessary and identify by block number)

Summary

An optical shearing technique has been used to produce high quality strain contours of centrally loaded, or thermally stressed and clamped plates. An analysis of strain from these fringes provides good agreement between experimental and theoretical values. It has also been shown that this technique is compatible with infrared thermographs in the detection of delamination in a composite laminated plate.

The above work was followed by developing an 'on-line' electronic speckle shearing technique in which the optical camera was replaced with electronic camera and its associated data storage and analysis and display system. This latter method shows good promise. However, it requires further work and equipments for better image process facilities to improve the fringe resolutions.

20. DISTRIBUTION/AVAILABILITY OF ABSTRACT	21. ABSTRACT SECURITY CLASSIFICATION
☐ UNCLASSIFIED/UNLIMITED ☐ SAME AS RPT. ☐ DTIC USERS	unclassified

22a. NAME OF RESPONSIBLE INDIVIDUAL	22b. TELEPHONE (Include Area Code)	22c. OFFICE SYMBOL
Dr Jqbal Ahmad	(01) 409-4423	AMXRM

SHEAROGRAPHIC IMAGING SYSTEMS

U.S. ARMY - ERO

CONTRACT NO. DAJA 45-84-C-0042

FINAL REPORT (May 1987)

Dr. D.K. Das-Gupta,
School of Electronic Engineering Sciences,
University College of North Wales,
Dean Street,
Bangor, Gwynedd. LL57 1UT

Summary

An optical shearing technique has been used to produce high quality strain contours of centrally loaded, or thermally stressed and clamped plates. An analysis of strain from these fringes provides good agreement between experimental and theoretical values. It has also been shown that this technique is compatible with infrared thermographs in the detection of deflamination in a composite laminated plate.

The above work was followed by developing an 'on-line' electronic speckle shearing technique in which the optical camera was replaced with electronic camera and its associated data storage and analysis and display system. This latter method shows good promise. However, it requires further work and equipments for better image processing facilities to improve the fringe resolutions.

1. Introduction

Non-destructive measurement of strain, stress and bending movements need to be made since these parameters provide information on strength, safety and lifetime of mechanical structure of materials and components. Strain is a kinematic quantity related to the derivatives of displacement. Stress and bending movents can be inferred from strain measurements and Hookes'law of elasticity. Strain is also a tensor quantity requiring nine components for its complete specification. Six of these components are independent, consisting of three components of normal strain (i.e., change in length per unit length of a small element in each co-ordinate direction) and the remaining three representing shear strain.

A determination of strain requires a differentiation of a measured distribution of surface displacements. A direct numerical differentiation may be made using a finite difference approximation and then fitting an interpolating polynomial to the data. The accuracy is seriously limited in this method as experimental error is magnified during the differentiation process.

Alternatively, optical differentiation (i.e. Moiré differentiation) may be employed which has the advantages of obtaining results which provide a visual display of strain. However, Moiré fringe technique tends to demand stringent requirements of absence of vibration and rigid body rotation. Now Shearography is a speckle shearing technique, developed recently [1-5], which also allows a direct measurement of displacement gradient (strain) and it does not require the stringent requirement of Moiré technique, mentioned above.

2. Shearography (The Speckle Shearing Technique)

Shearography employs a coherent light source (figure 1) to illuminate the surface of an object which may suffer an out-of-plane displacement due to the application of a mechanical or a thermal force. The reflected beams from this surface are imaged with an optical camera which has a small angle optical wedge covering half the field in the iris plane of the image forming lens of the camera. The glass wedge

(i.e. prism) deviates the incident path of a ray and thus two laterally sheared images, (focussed by each half of the lens), P_1 and P_2 of the object point P(x,y) are formed. This shearing occurs (say) in the x-direction for a ray travelling in the z-direction. If two neighbouring points P(x,y) and P(x+dx,y) are now considered (figure 2), for the correct wedge orientation in the x, z plane, the rays from the two point sources will meet at the same spatial location in the image plane. If there is any out-of-plane displacement (i.e. backwards or forwards), then the rays will move apart and shearing δx, will be produced which, for unit magnification, is given by:

$$\delta x = D_i (\mu - 1) \theta \qquad \ldots (1)$$

where D_i is the image distance, i.e. the distance from the object to the wedge, μ the refractive index of the glass wedge and θ the wedge (i.e. prism) angle.

The photographic plate in the image plane is double exposed with the object being stressed between the exposures. If the object is deformed under stress, an optical path change occurs due to surface displacement of the object which provides a phase change Δ between the two sets of sheared wave fronts, where,

$$\Delta = (2n + 1)\pi \qquad \ldots (2)$$

where n is the fringe order and the dark fringes occur with 1,3,5 7 ... (odd orders). Thus the resulting intensity distribution on the photographic plate after double exposure thus provides a speckle sheared fringe pattern. Although these fringes are visible with non-linear photographic recording, a high contrast fringe pattern, however, can be obtained by blocking the zeroth-order spectrum using Fourier filtering. Figure 3 shows typical 'Bull's eyes' speckle sheared fringes of a centrally loaded rectangular metal plate which was obtained in the present work.

3. Experimental

The optical arrangement for the production of a shearogram is shown in figure 4. A He-Ne laser (Spectra-Physics, type 125A) of wavelength 0.633 μm and 50 mw power was used as a coherent radiation source throughout the project. The laser was provided with an external exciter (spectra-physics model 261) in order to keep all heat generating components isolated from the optical resonator, thus providing good thermal stability which is of importance. The laser beam is spatially cleaned by x40 microscope objective lens and a 30 μm aperture arrangement in order to provide a clear Gaussian intensity profile. This 'clean' beam is then expanded sufficiently to span the width of the sample. In the present arrangement, the beam is incident on the sample surface at angle of approximately 30 degrees, the reflected beam being always normal to the focussing lens of the optical camera. A Toyo-view camera (Model 45E) in conjunction with a Schneider -Kreuznach symmer S150 mm, F5.6 compound lens has been used in this work. The optical wedge, located in the iris plane of the camera lens, consists of one-half of a circular glass disc (type Bk7, refractive index 1.517642), the other half being plane parallel and of uniform geometry. The angle of the wedge is 1 degree.

Figure 5 shows schematically the sample holder arrangement in which a load cell has been incorporated (ELF 1000) in series with a displacement pointer and a micrometer (Mitatoyo) head. The load cell is connected to a digital voltmeter which is designed to give a full scale 250 mV output for a range of 0-1 kg load.

There was a 15 minute warm-up time for the load cell and re-zeroing was necessary after every load change. Also included in this arrangement is a battery operated LED circuit which provides an identification when the displacement pointer is just in contact with the sample located in its holder. The micrometer device is capable of measuring accurately a minimum out-of-plane displacement of 1 μm and the load cell is able to measure a minimum load of ~0.5gm. The test samples employed in this

work were discs of stainless steel and brass (0.3 mm thickness each) and and PMMA of 1.8 mm thickness and 80mm in diameter. The surface of the disc was sprayed matt white using cellulose based paint to increase the surface reflectivity. Also drawn on the white surface were two fine intersecting lines in the horizontal and vertical planes respectively. The sample was mounted in the central cut out of the sample holder (Figure 5). The sample surface was at first imaged by the Toyo-view camera for zero displacement on a photographic plate (type Agfa-Gevaert Holotest 10E75), the exposure time being 5s when the separation of the laser and the sample and the camera were 73 cm and 26 cm respectively. The camera apurture was set at f5.6 throughout the experiment. With the camera plane normal to the surface, the image was first adjusted to give an approximate 1.1 magnification, thus reducing the effects of lens aberrations. The image shearing wedge was adjusted so that no shearing of the horizontal line was present, thus allowing shearing only in the vertical direction. The laser was allowed to warm up for an hour before exposures were made. Over a period of five hours, the power drift of the laser was approximately 5%. A second exposure of five seconds was then made on the same photographic plate after providing an out-of-plane displacement by a specific magnitude in the range of 2-80μm. The double exposed plate containing the original shearogram was then developed (Ilford PQ) for 8 minutes and fixed (Hypam) for a further 10 minutes. Emulsions are prone to swelling and shrinking during development. Changes in thickness of the emulsion may result in a phase shift giving a loss of diffraction efficiently. Non-uniform swelling or shrinking can also occur during developing and fixing. Thus it is necessary to have as short a developing and fixing time as possible. This can be done by over-exposing the plate and under-developing it.

The sensitivity or speed of emulsion is determined by the size of the silver halide grains, the larger grains being more sensitive than the smaller ones. The reason for this is that the incident light frees electrons which are then trapped, thus becoming available for reducing

a mobile silver ion to silver atom which absorbs light strongly giving high gain and sensitivity. The films employed in this work can resolve down to 0.2 μm giving 1500 lines per nm which makes it ideal for Holographic work.

The reconstruction of the shearogram was performed using the original plate as the object and the optical arrangement is shown in figure 6. In this case, the optical wedge was removed from the iris plane of the Toyo-view camera. An apurture of 4mm in diameter and displaced by 8mm from the central optical axis way located in front of the camera to provide high pass Fourier filtering. For reconstruction an exposure time of 8 seconds has been found suitable in general.

4. Results and Discussions

4.1 Mechanical Loading and Out-of-Plane Displacement

Figure 7 shows a typical set of reconstructed shearograms of a stainless steel plate with an out-of-plane displacement of 12 μm which was obtained by imaging and Fourier filtering of an original double exposed photographic plate containning a speckle sheared fringe pattern, obtained at unity magnification. Also on the shearogram is superimposed a sheared image of a reference grid line. Figures 7(a) - 7(f), 8(a) - 8(f) and 9(a) - 9(f) show the shearograms with out-of-plane displacements in the range 10 μm - 43μm for stainless steel, brass and PMMA plates respectively. Since the fringes are symmetrical, only one half of each set is shown in these figures (7-9) for brevity.

These figure patterns represent the derivative of the displacement component in the z-direction with respect to the x-coordinate, i.e. $\delta w/\delta x$. For normal illumination and viewing, placing the origin of the coordinate system between the two symmetric lobes as seen in figure 6, it may be shown [1-5] that:

$$\frac{\delta w}{\delta x} = \frac{\Delta\lambda}{4\pi\delta x} = \frac{(2\eta+1)\lambda}{4\delta x} \qquad \ldots (3)$$

where Δ is given by equation 2, λ is the wavelength of the incident coherent laser light and δx is given by equation 1. Thus the values of $\delta w/\delta x$ may be evaluated from equation 3 using the experimental data.

Now the deflection (in the z-direction), of a clamped circular plate loaded at the centre is given by[7]:

$$w(s) = \frac{Ps^2}{8\pi D} \ell\eta \frac{S}{R} + \frac{P}{16\pi D} (R^2 - S^2) \quad \ldots (4)$$

where s is the distance from the centre, P the total load applied, R the plate radius. D is the flexural rigidity of the plate and is given by :

$$D = \frac{Eh^3}{12(1-\rho^2)} \quad \ldots (5)$$

where E is the modules of elasticity of the material and ρ the Poissons ratio and h the plate thickness. Differentiating equation 4, we get:

$$\frac{dw}{ds} = \frac{PS}{4\pi D} \ell\eta \left(\frac{S}{R}\right) \quad \ldots (6)$$

Thus the theoretical values of dw/ds may be calcualted using equation 6 and compared with experimentally observed values of $\delta w/\delta x$ (equation 3) in order to establish the suitability of shearographic system for the out-of-plane strain as a non-destructive method. Table 1 gives the values of modules of elasticity E, and the Poisson's ratio for the three materials (i.e., stainless steel, brass and PMMA) and in the present work.

Table 1 Material Constants

	Stainless Steel	Brass	PMMA
E(psi)	28×10^6	14×10^6	0.4×10^6
ρ	0.30	0.33	0.4

The amount of shearing δx was measured directly from the sheared reference grid lines on the plate. The fringes were then numbered, the dark fringes being integer values of n and bright fringes being n/2. The co-ordinate system was placed centrally between the two lobes of the pattern and fringe positions were measured. Thus the stress of individual fringe positions were calculated and compared with theoretical values using equations 3 and 6. Some typical results of these calculations are shown figures 10(a) and 10(d) for stainless steel, figures 11(a) and 11(b) for brass and figures 12(a) - 12(d) for PMMA plates in which stresses against distances from the centre have been plotted. As is expected, the largest gradient corresponding to the largest displacement is at the centre of the plate. Also when the distance from the centre is equal to the radius of the sample, no gradient is expected since it is clamped at this point. The maximum strain and hence stress were found to occur

at 0.8 cm, 1.25 cm and 1.25 cm from the centre, for stainless steel, brass and PMMA samples respectively. Rather surprisingly, this was not found to be significantly sensitive to flexural rigidity.

For small displacements, few fringes were produced so the agreement between the theory and practice is not as good as with fringes obtained with increasing displacements. The discrepancies between experimental and theoretical results can be attributed to not being able to accurately defining the sample boundaries. Using adhesive as a method of clamping means that the effective radius of the sample varies between 35–40 mm around the perimeter. The uncertainty in radius R, of the sample was found to have a significant effect on the calcualted stress values in comparison with the uncertainties in x, D and P. Nevertheless, the results show good agreement between the experimental and calculated values in most cases for out-of-plane displacements provided by mechanical loading (forces) of the samples.

4.2 Thermal Stressing

On heating a clamped plate internal stresses are developed which are compressive on the warmer side and tensile on the cooler side. The surface stress Γ_T is given by:

$$\Gamma_T = \frac{E\alpha\Delta T}{2(-\rho)} \qquad \ldots (7)$$

ΔT is the temperature difference between the two sample surfaces, α is the thermal expansion coefficient of the material, the other symbols have been defined earlier. In the steady state the thermal stress is proportional to ΔT and and independent of sample thickners. Under transient conditions, initially the temperature gradient is confined to a thin layer of the surface and the initial stress is $2\Gamma_T$ before equilibrium is reached.

In this work an 18W heating element was applied to a 270μm thick stainless steel sample, 8 cm in diameter. An exposure was taken of the sample which was initially heated for 30s and then a second exposure was made after further heating of the samples for an additional period of 90s. Figure 13 shows the strain contours of the thermally stressed sample. The temperature change in this case is estimated to be approximately 6^0 c assuming that the glue acted as a perfect insulator and that the heat was distributed uniformly. The fringes are not as sharp as those with mechanical loading probably due to the fact that the sample temperature was changing during the five second exposure time.

Further experiments with thermal stressing were made at the U.S. Army Materials Technology Laboratories (Watertown, Ma) using a graphite epoxy, ten layer, cross ply, laminated plate in which teflon flaws were embedded in between different layers (see figure 14) in order to study shearographic delamination detection abilities. In this case, a heat lamp was used at the back of the laminate to induce thermal deformation. In order to reduce the exposure time and thus freeze the plate's thermally deformed state, a Ruby pulsed laser of 15-30 ns pulse width was used instead of the He-Ne continuous laser. Figure 15 shows sharp displacement gradient contours which were obtained by this technique. Figure 16 shows an infrared thermogram of the same graphite epoxy plate which was produced by heating the sample from one side with a high intensity pulsed Xenon lamp. As in the case of shearogram, the flaws closest to the surface may be detected by the thermographic technique.

Thus, it may be stated that optical shearography provides high quality displacement gradients (strain) contours with centrally loaded and thermally stressed clamped plates. The quality of this technique for delamination detection is comparable to that of infrared themography.

The next stage is to replace the optical camera with electronic camera and data storage and analysis equipments to provide on-line (real-time) display of strain i.e. electronic speckle shearing technique.

5. Electronic Speckle Shearing System

The on-line electronic speckle shearing system has obvious advantages in detection of strain in a non-destructive manner, although its resolution will be reduced from more than 100 lines/mm for holographic emulsions to 500 lines resolution of TV image. The electronic system comprises of three components, i.e. (i) optics to form the image, (ii) a photo-active surface to detect the image (active area 12x10mm) and (iii) scanning electronics (625 lines at 25 frames per second for PAL and 525 lines for NTCS) to read the electronic image. The small angle optical wedge in this system is located at the iris plane and the optical lens associated with the electronic camera. The video camera provides an electronic charge which is proportional to the intensity of the image and the photo-sensitive layer of the camera phase plate is scanned by an electron beam thus generating an output voltage, i.e., an electronic equivalent image. Figure 16 shows schematically an 'on-line' shearographic system using electronic processing. Here the video signal of the speckle sheared pattern of the unstressed object is stored digitally. The object is then stressed in the video signal ofthe stressed object and then subtracted from the stored signal of the unstressed sample. The output is then high pass filtered and rectified and displayed on the monitor. Those areas of the two images where the pattern remains uncorrected give zero dark fringes and correlated images give non-zero bright fringes. It may be shown that for the subtracted image the brightness B (averaged along a line of constant phase change, A), varies between maximum and minimum values B_{max} and B_{min}, where,

$$\left.\begin{aligned} B_{max} &= (2\eta+1)\pi, \qquad \eta = 0,1,2 \quad \ldots \\ B_{min} &= 2\eta\pi, \qquad \eta = 0,1,2 \quad \ldots \end{aligned}\right\} \quad (8)$$

A comparison of equations 8 and 2 shows that fringes obtained by this method are identical to those obtained optical photographic correlation.

In general, subtracted signals have negative and positive values. The video monitor sees, however, negative signals as areas of blackness. Hence, the subtracted signal is rectified before it is displayed on the monitor. A high-pass filtering of the signal improves the visibility of the fringes by removing low frequency noise, together with mean speckle intensity variations, thus enhancing the fringe clarity.

6. Electronic Speckle Shearing Experiments

With the above in view, a modified 'Vidispeck' electronic stress analysis and data display system was purchased from Ealing Electro-Optic plc. of the U.K. The original 'Videospec' system is based on electronic speckle interferometer (ESPI) and not on speckle shearing technique. Furthermore, as stated earlier, we already had a 50 mW laser and we also purchased an MTI-Nuvicon electronic camera (type NC-68 with RS-330 sync., 2 interface, sync/Drive lock outputs) with a 54076 selected Grade 1 tube. Thus the modified 'Videospec' system did not have its laser and video camera and consisted of the electronic frame storage data subtraction and monitor units with analog output. The Nuvicon camera was used with a Micro Nikon 105mm optical lens at f16 and the optical wedge. Figures 17 and 18 show the fringe contours obtained with the electronic speckle shearing system for two different out of plane displacements for the PMMA plate using the present system. An IVS-200 system was used for digitising and processing of full frame TV imaging at 'real-time' speeds. The IVS syswtem has a special resolution of 512 x 512 pixels and a digital dynamic range 256 grey levels. Only two narrow bands of grey levels on either side of the central high intensity values were used to obtain these fringes. It seems to be necessary to expand the spatial resolution significantly, together with an increase of the dynamic range of the grey levels for improving image quality.

Further work on development of image processing will be required to establish a satisfactory 'on-line' Electronic Speckle shearing techniques for stress analysis. Present work, however, shows clearly that this technique has considerable potential in diverse applications in the non-destructive measurement of deformation and strain.

References

1. Y.Y. Hung and A.J. Durelli, J. Strain Analysis, 14, 81 (1979)

2. Y.Y. Hung, Optical Engineering, 21, 391 (1982).

3. Y.Y. Hung and C.E. Taylor, Proc. Soc. Photo-Opt Inst. Engng., 17th Annual Tech. Meeting, 41, 169 (1973).

4. Y.Y. Hung, I.M. Daniel and R.E. Rowlands, Exp. Mech., 18, 56 (1978).

5. Y.Y. Hung, 'Speckle Metrology'. Ed. R.K. Erf, Academic Press p.p. 51-71 (1978).

6. D.K. Das-Gupta, R.F. Anastasi, S.M. Serabian and R.J. Shuford SPIE: to be published 1987).

7. S. Timoshenko and S. Woinowsky-Kriegers, 'Theory of Plates and Shells', 2nd Ed., McGraw-Hill, N.Y., p5 and p69 (1959).

8. R.F. Anastasi, S.M. Serabian, R.J. Shuford and D.K. Das-Gupta Expt. Mech. to be published (1987).

9. R.J. Shuford, T.J. Murray, Y.L. Hinton and R.H. Brockelman, Composites in Manufacturing 4 Confrerence, anaheim, CA., Jan. 7-10 (1985).

10. R. Jones and C. Wykes, 'Holographic and Speckle Interferometry' Cambridge Univ. Press, Cambridge, U.K. Chapter 4, pp 165-197 (1983).

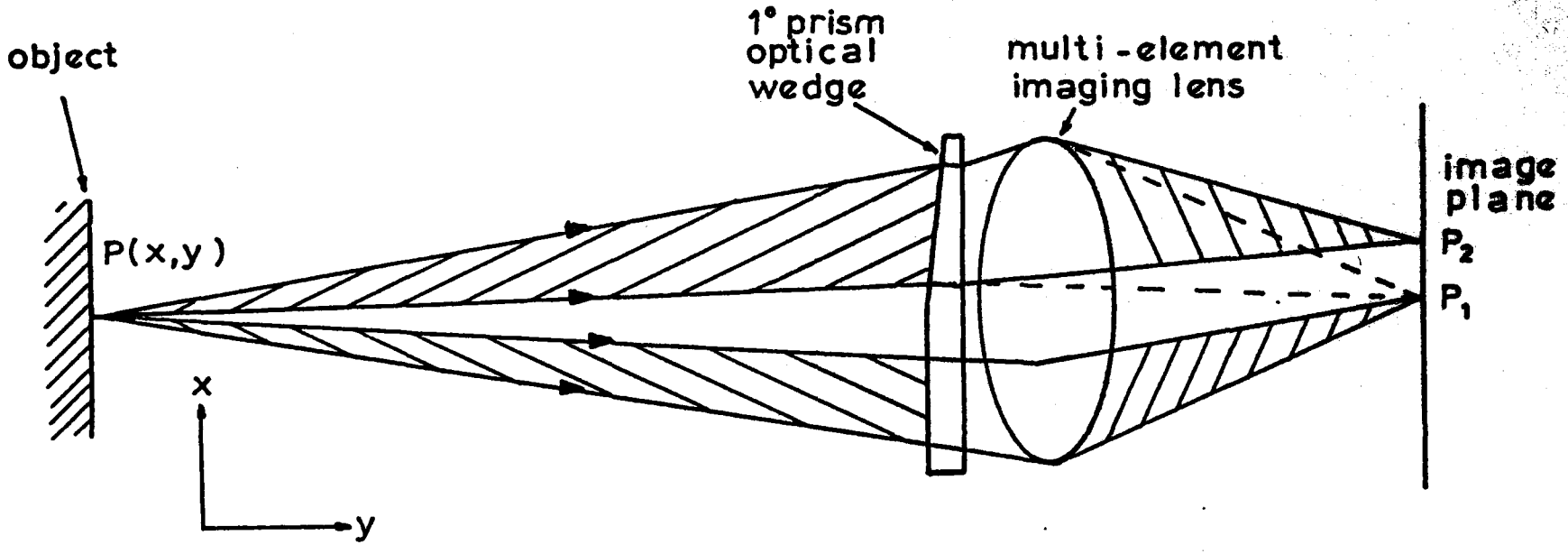

Figure 1. Schematic diagram of shearography.

FIG. 2: Rays from two points are brought to meet in the image plane

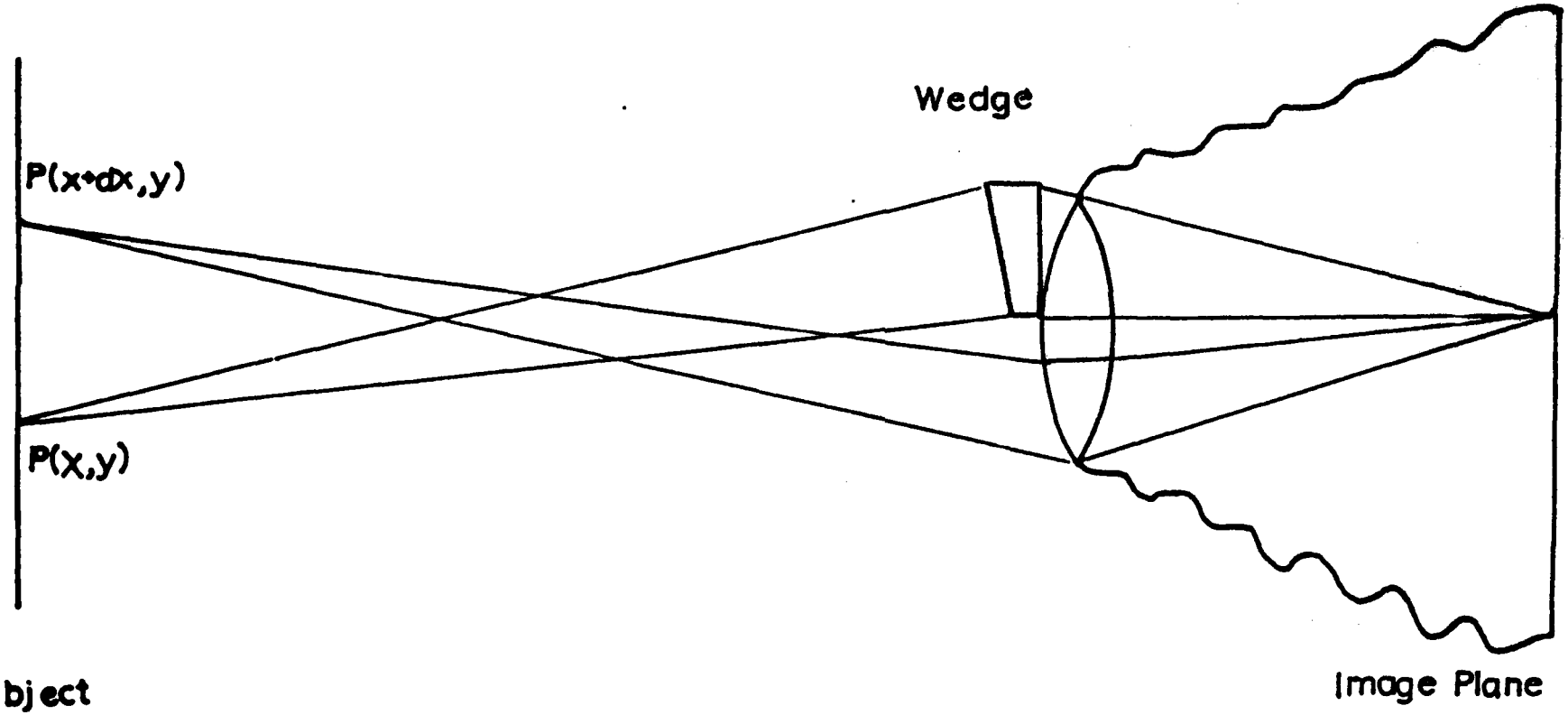

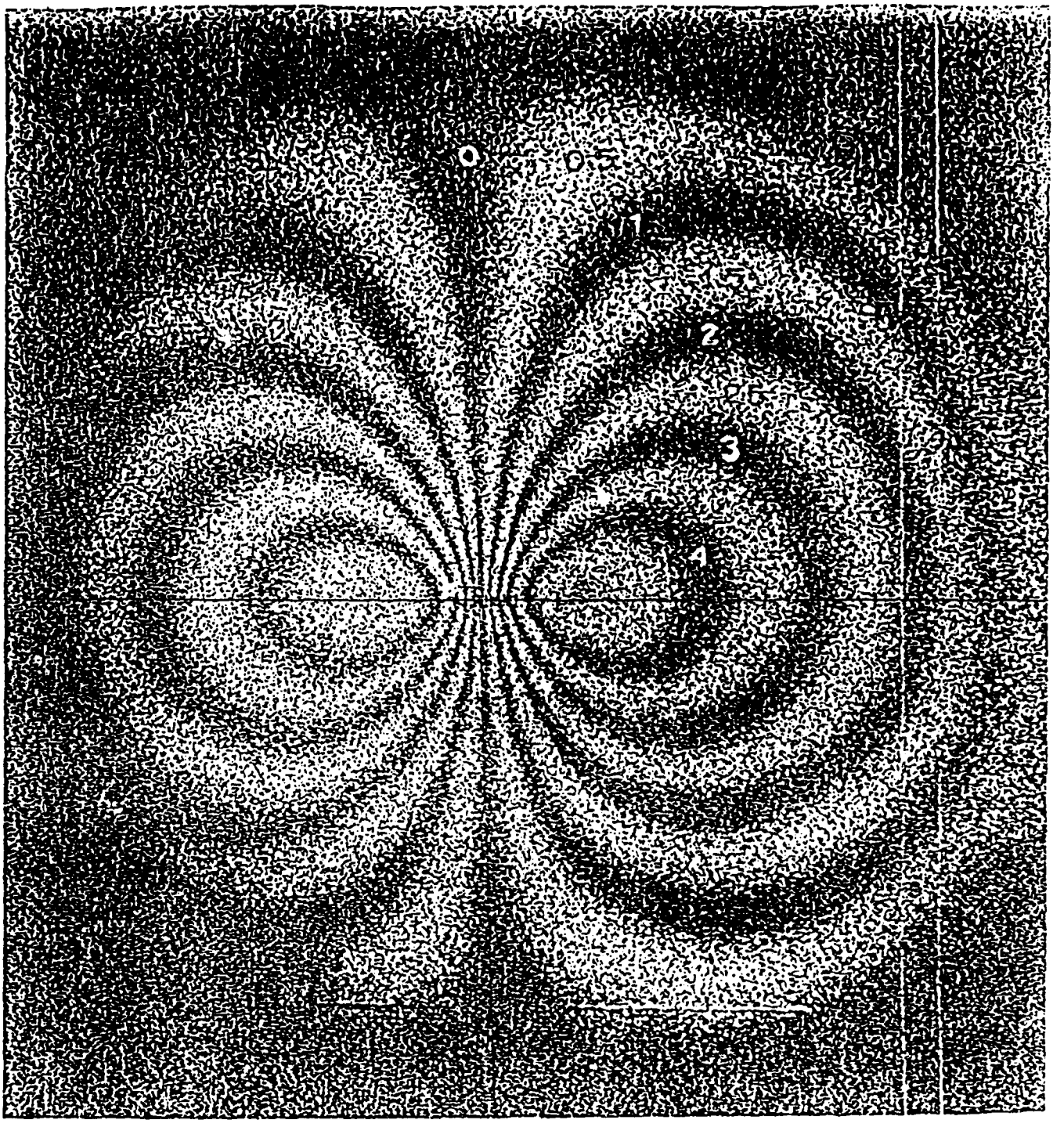

FIG. 3: Typical Fringe Pattern

Figure 4 . U.C.N.W. shearographic imaging system .

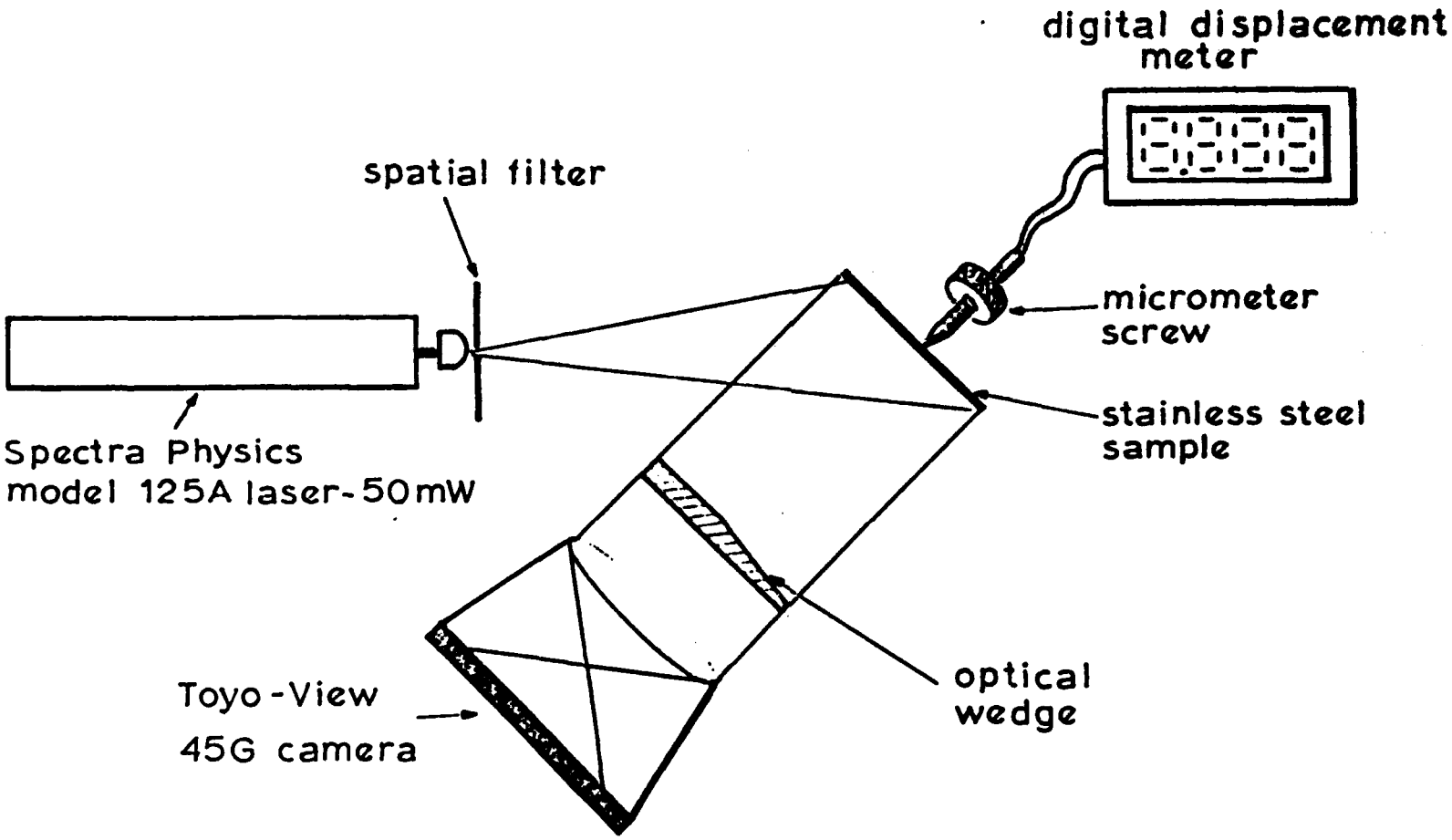

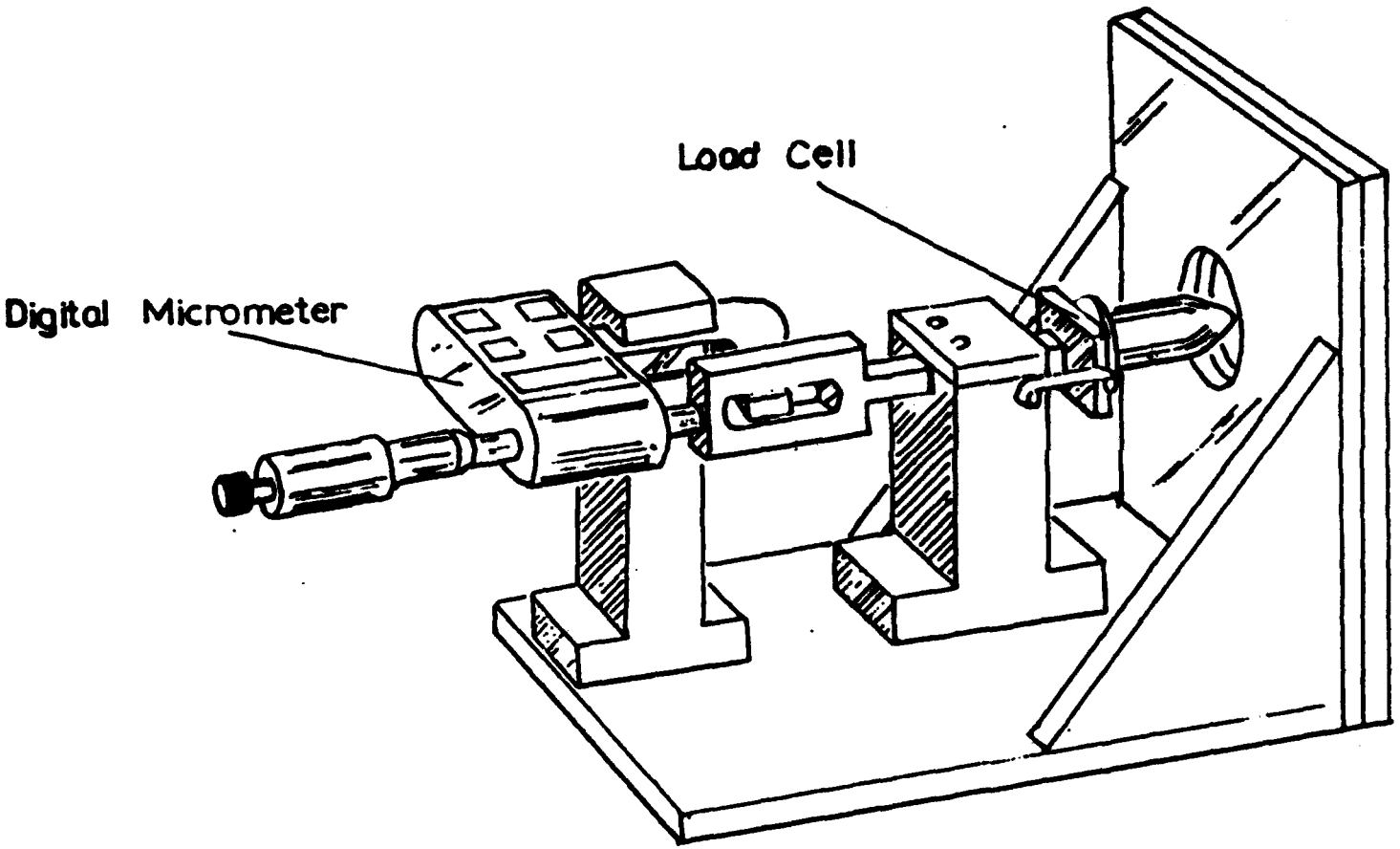

FIG. 5: Diagram of Sample Holder and Load Cell

Figure 6 . U.C.N.W. shearographic image reconstruction arrangement.

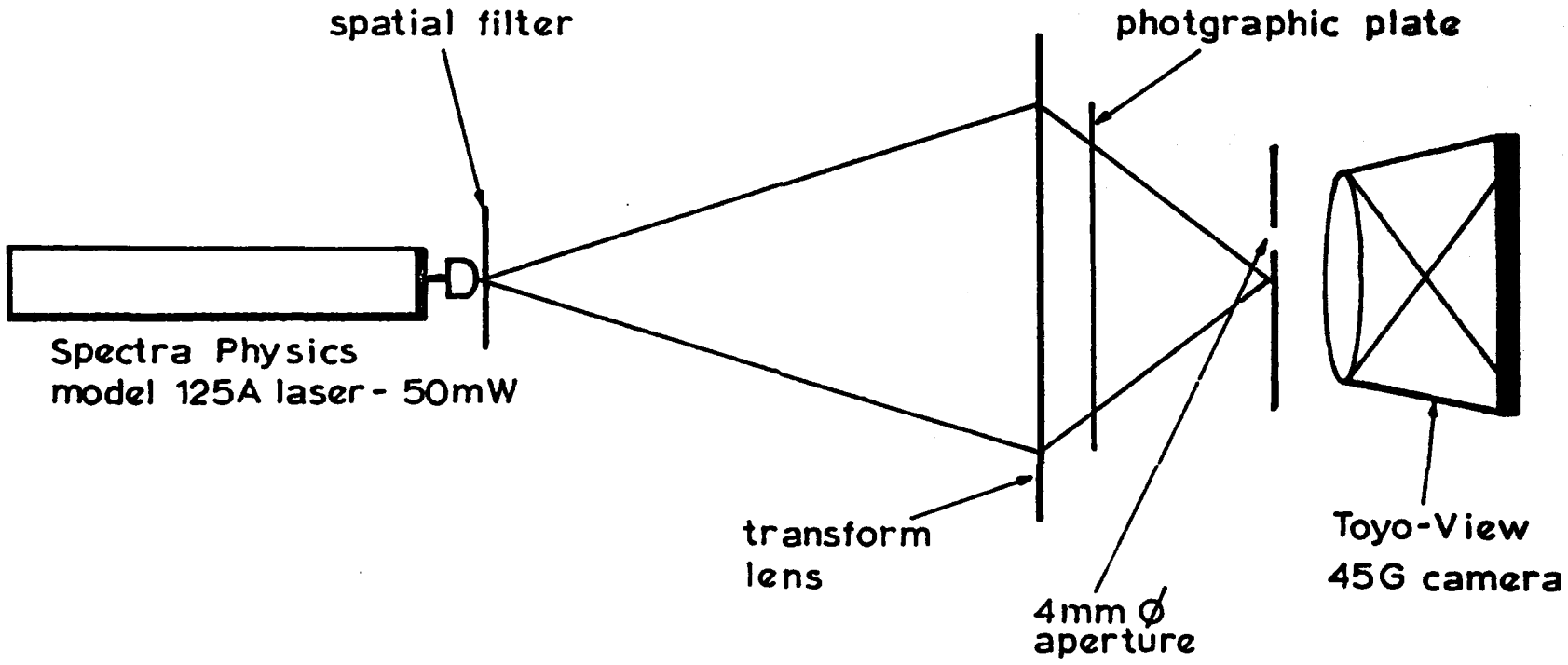

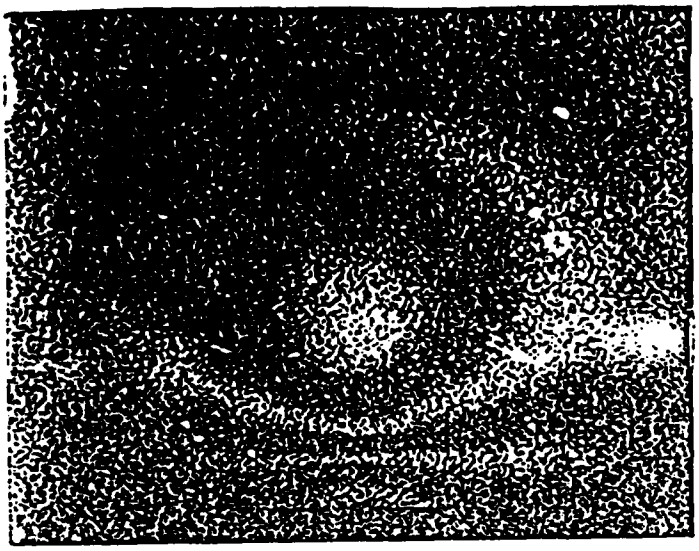

(a) 6 μm

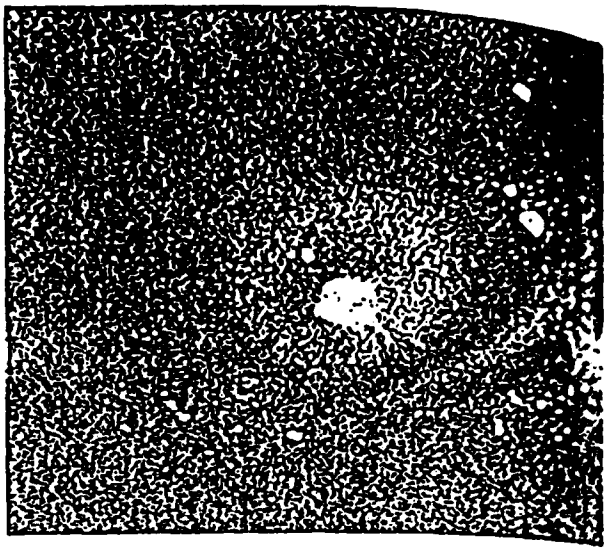

(b) 8 μm

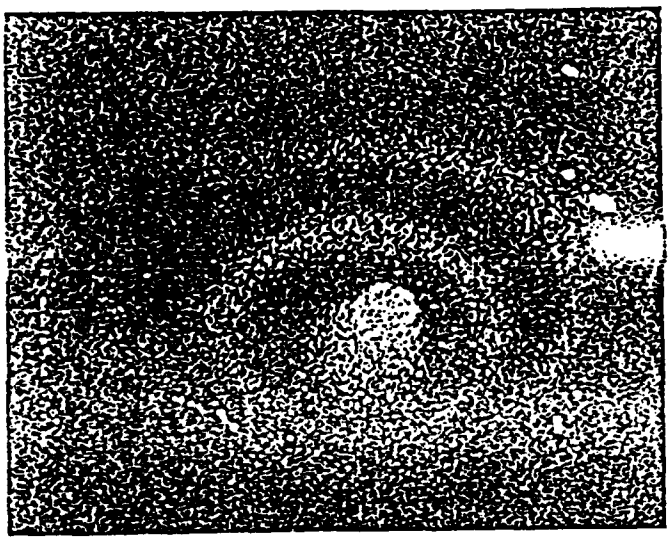

(c) 12 μm

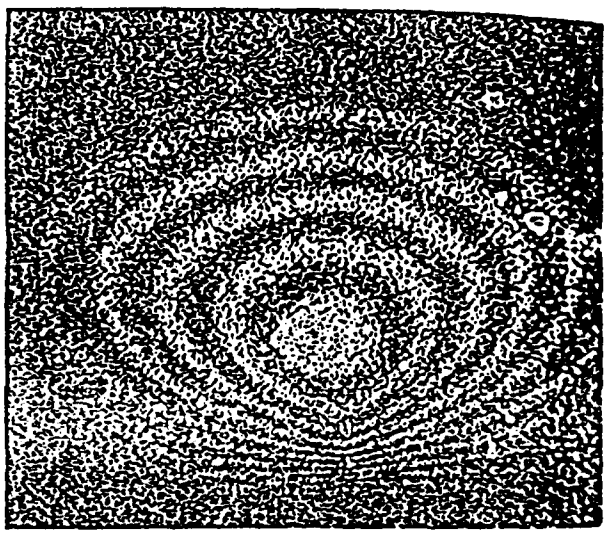

(d) 17 μm

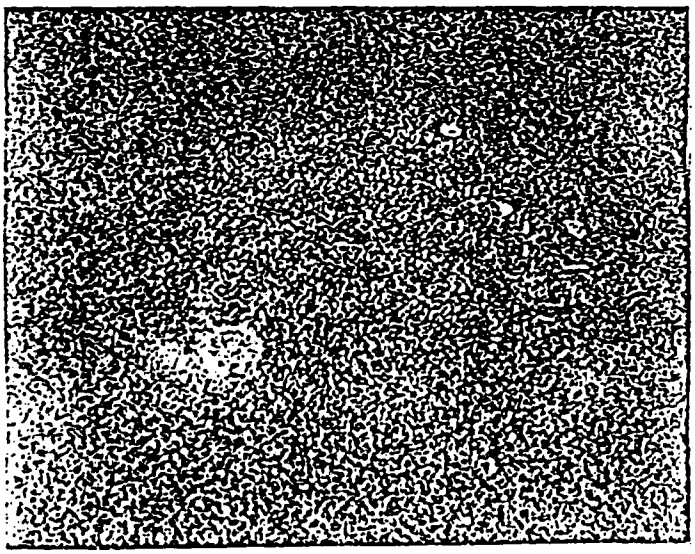

(e) 22 μm

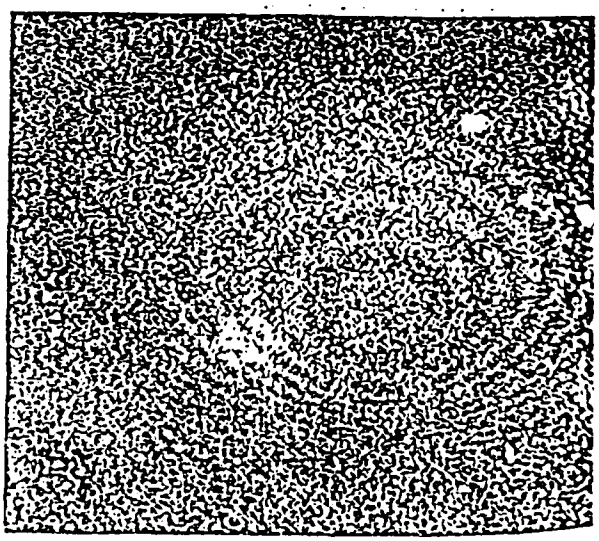

(f) 27 μm

FIG. 7: Steel Results

(a) 8 µm

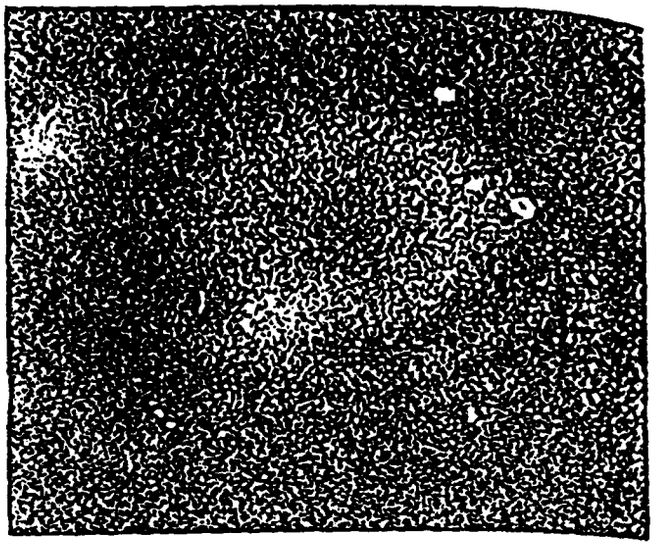

(b) 12µm

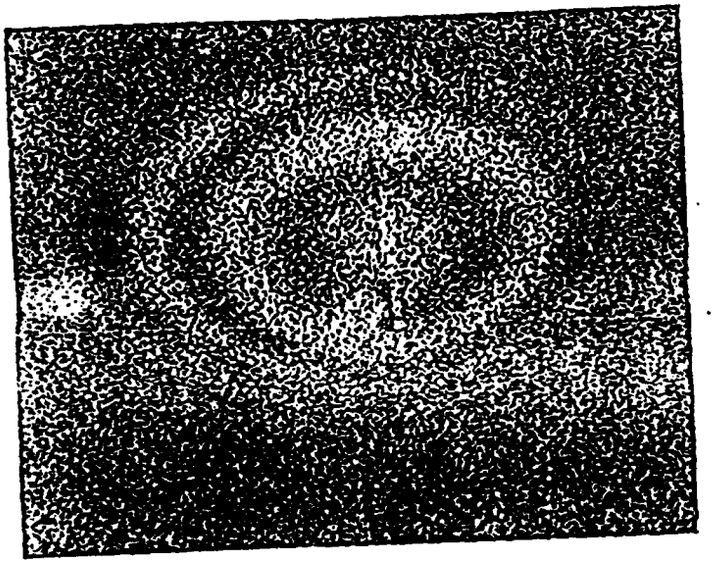

(c) 15 µm

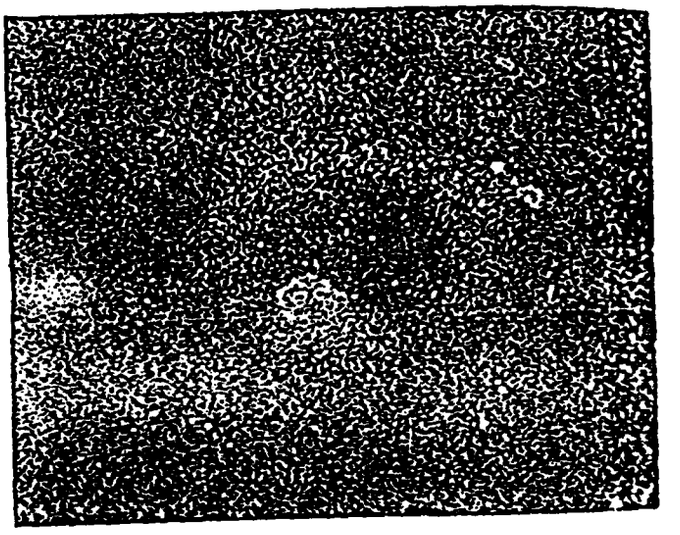

(d) 20 µm

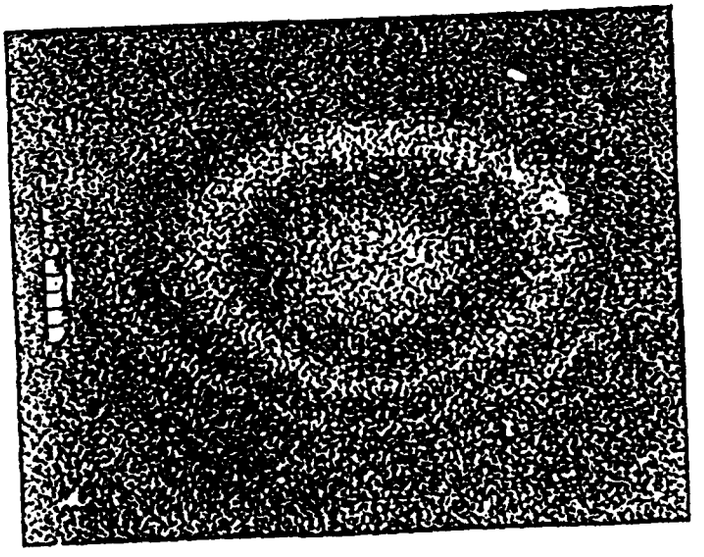

(e) 25 µm

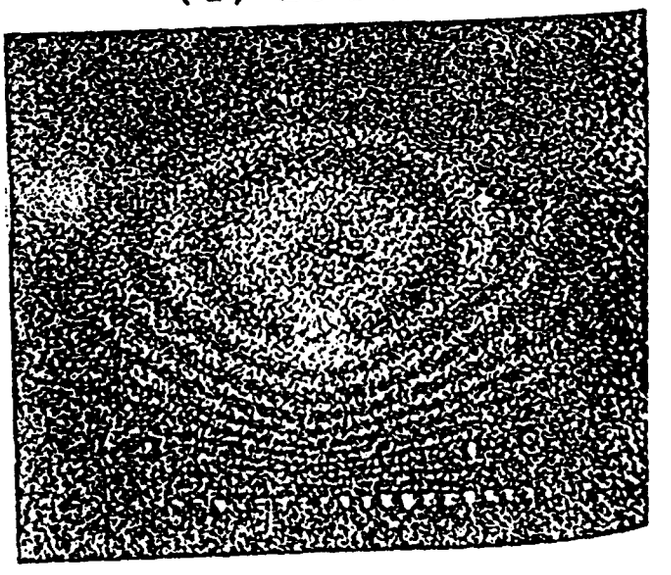

(f) 30 µm

FIG. 8: Brass Results

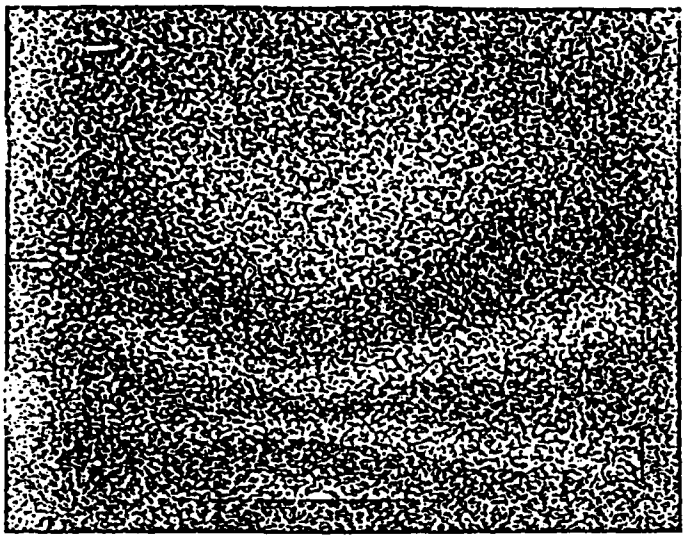

(a) 10 µm

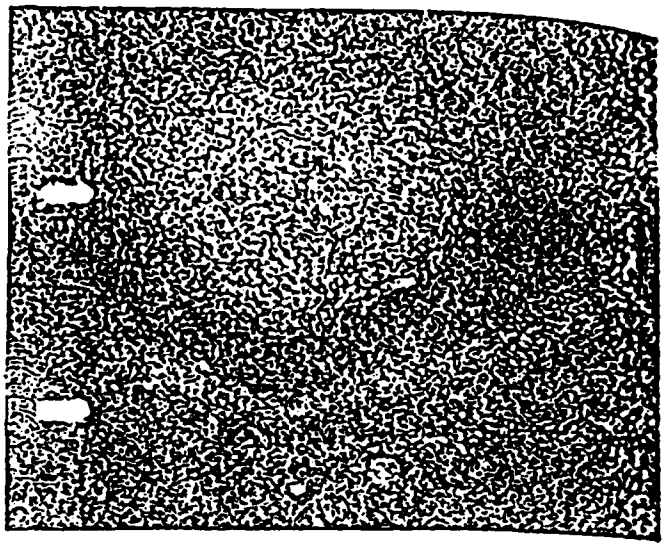

(b) 13 µm

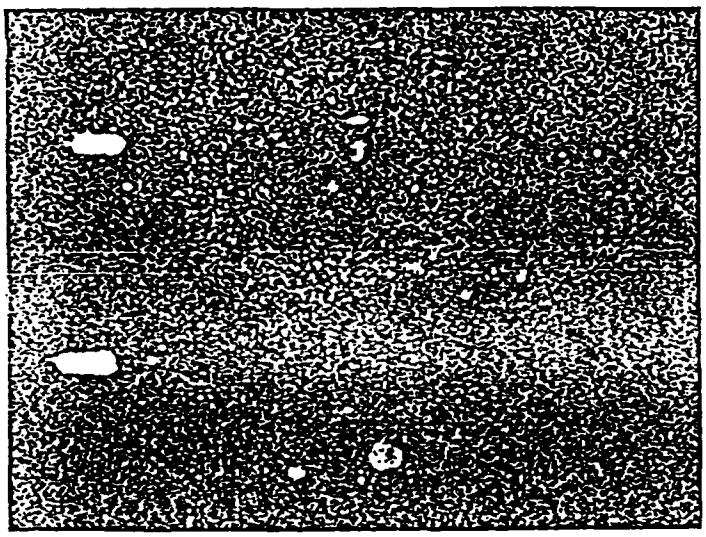

(c) 15 µm

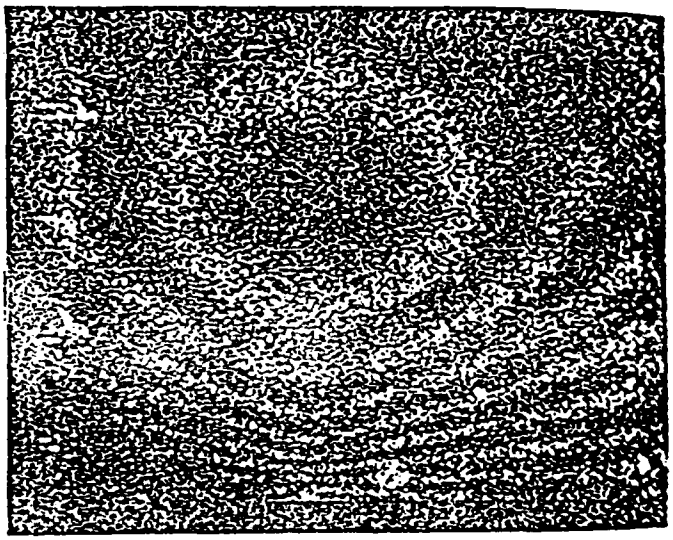

(d) 30 µm

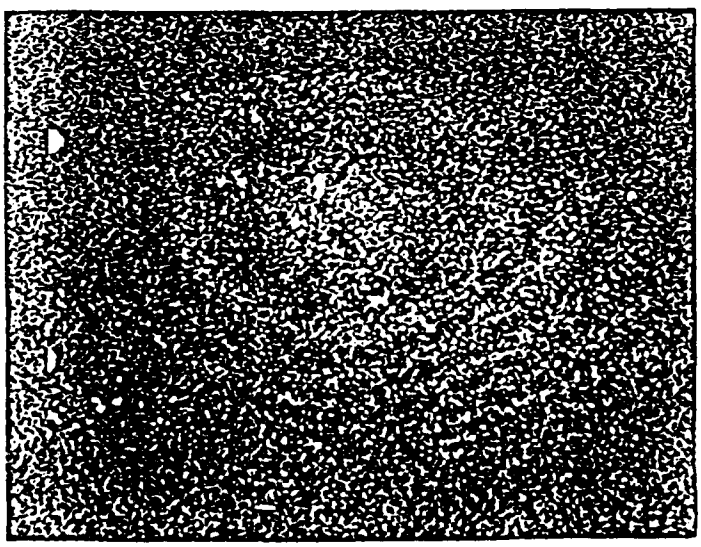

(e) 38 µm

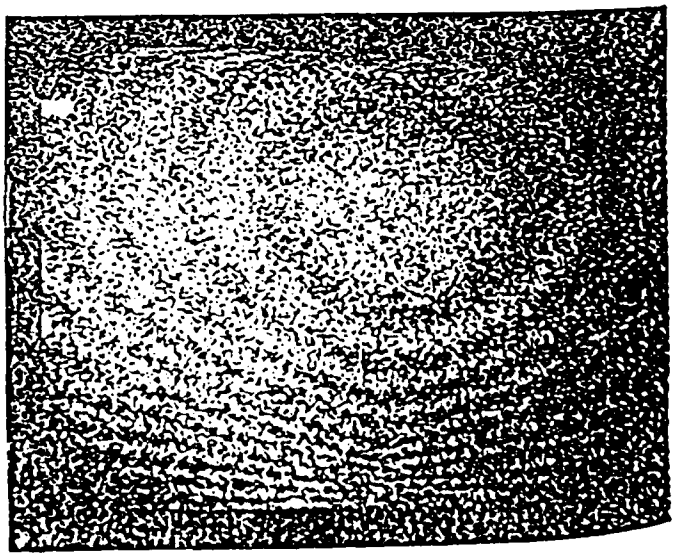

(f) 43 µm

FIG. 9: P.M.M.A Results

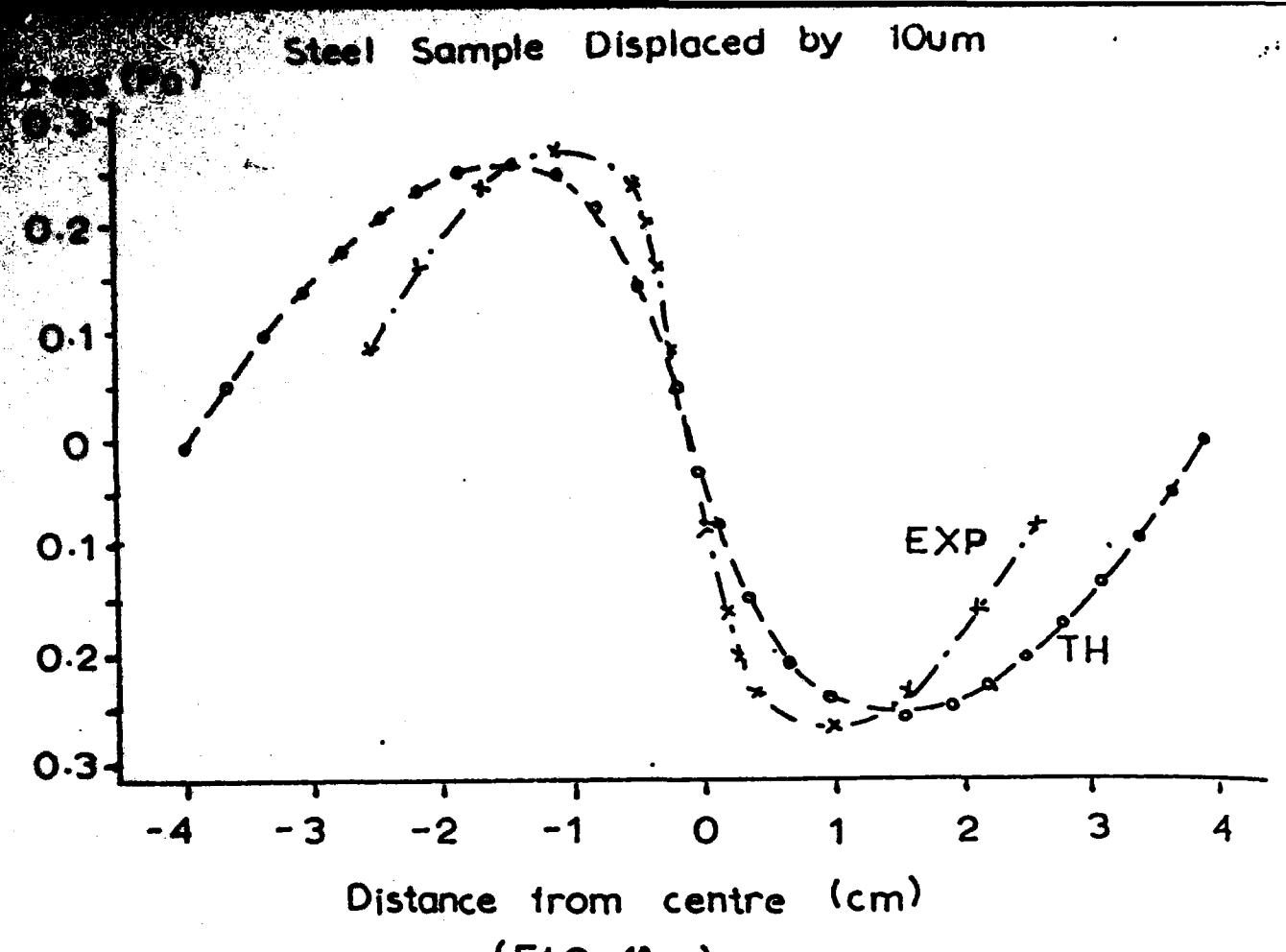

(FIG. 10a:)

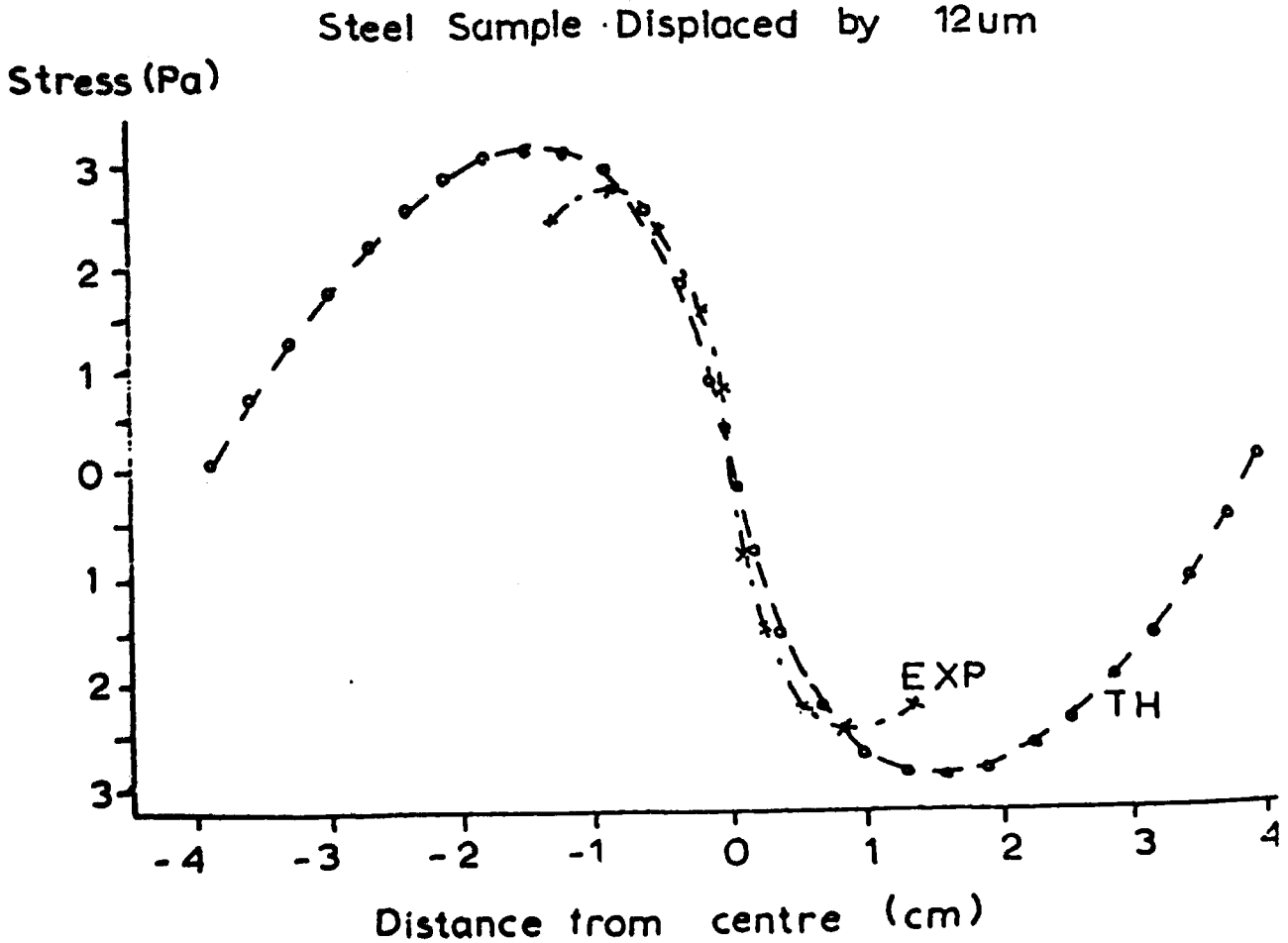

(FIG. 10b:)

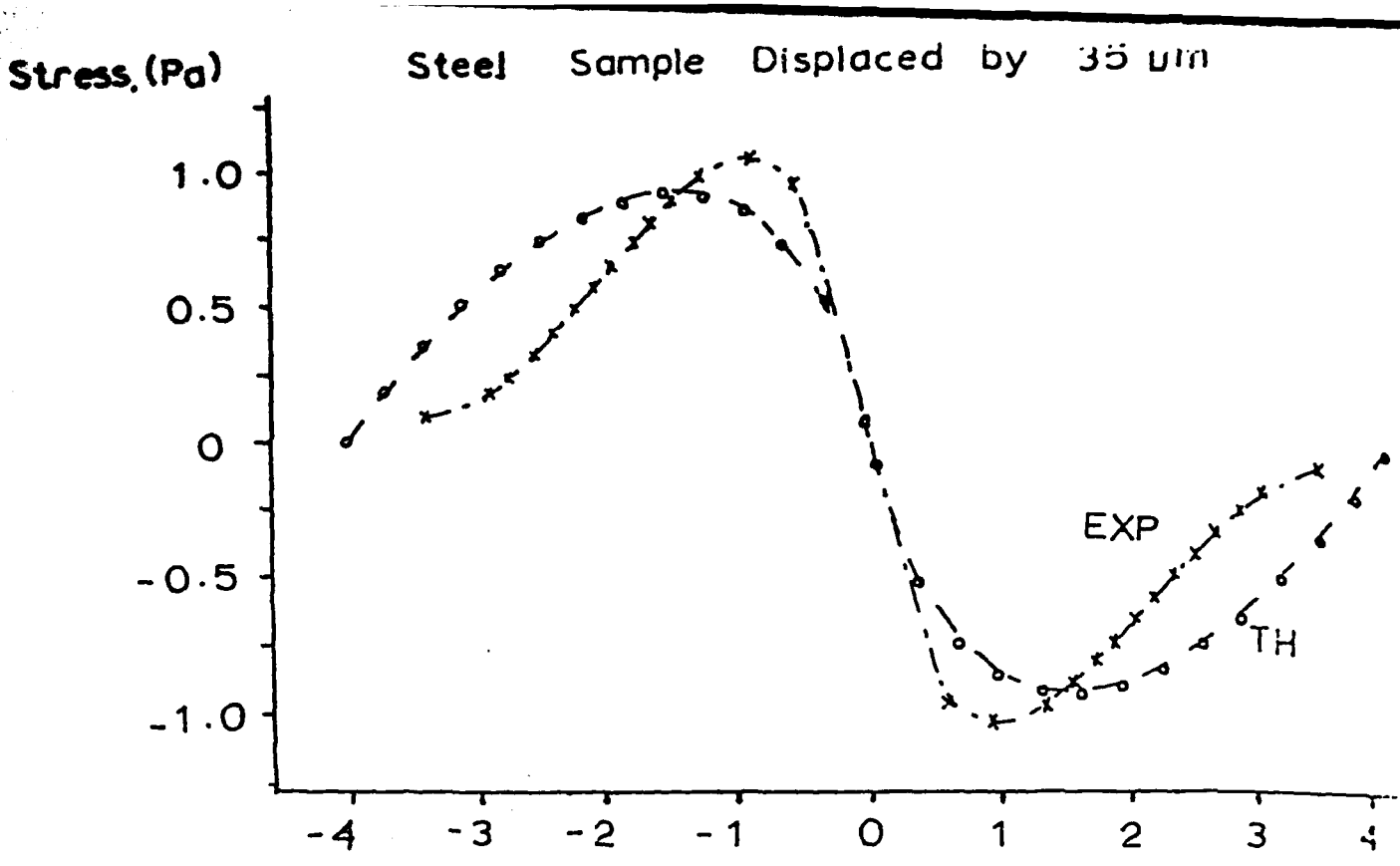

(FIG. 10c:)

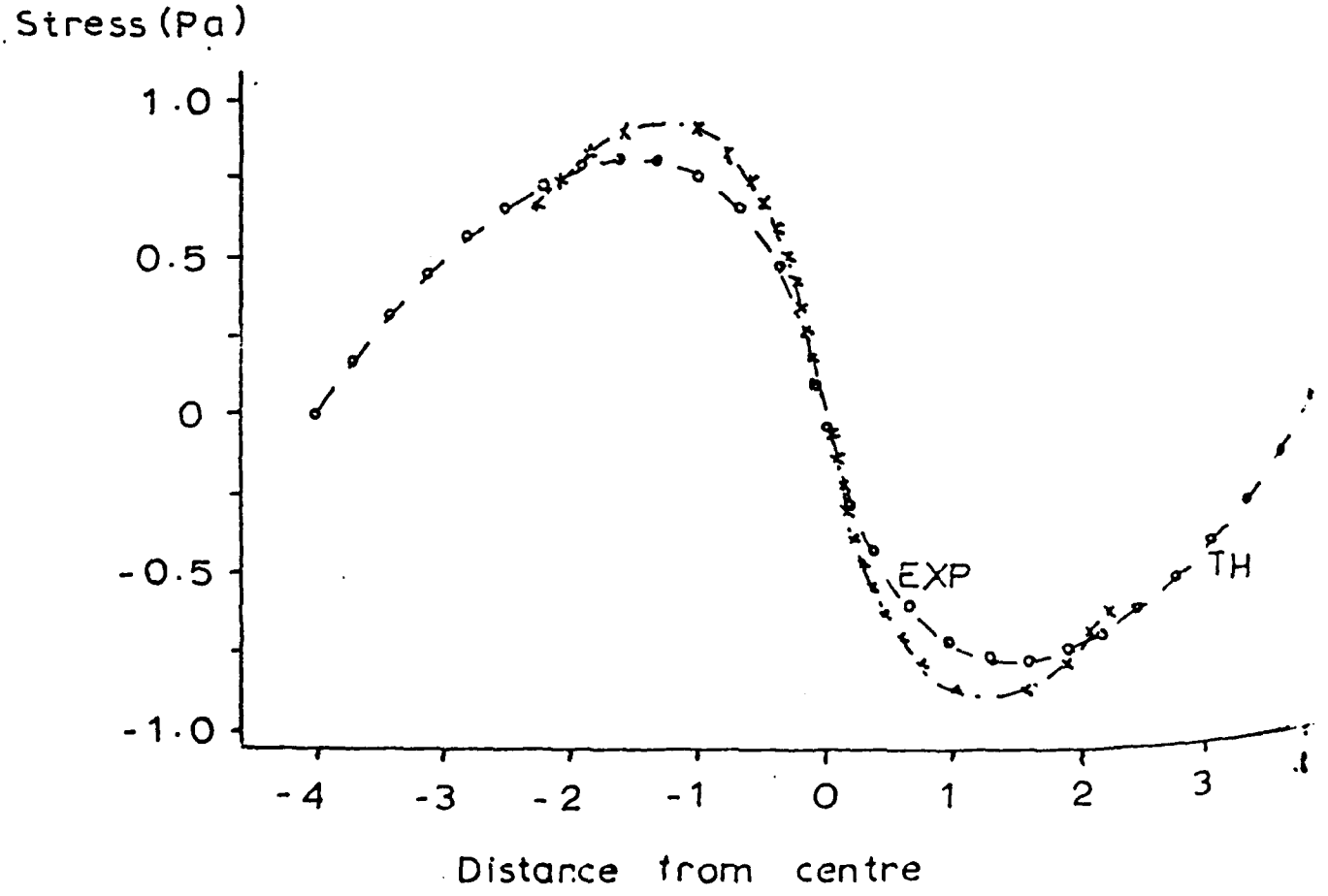

(FIG. 10 d:)

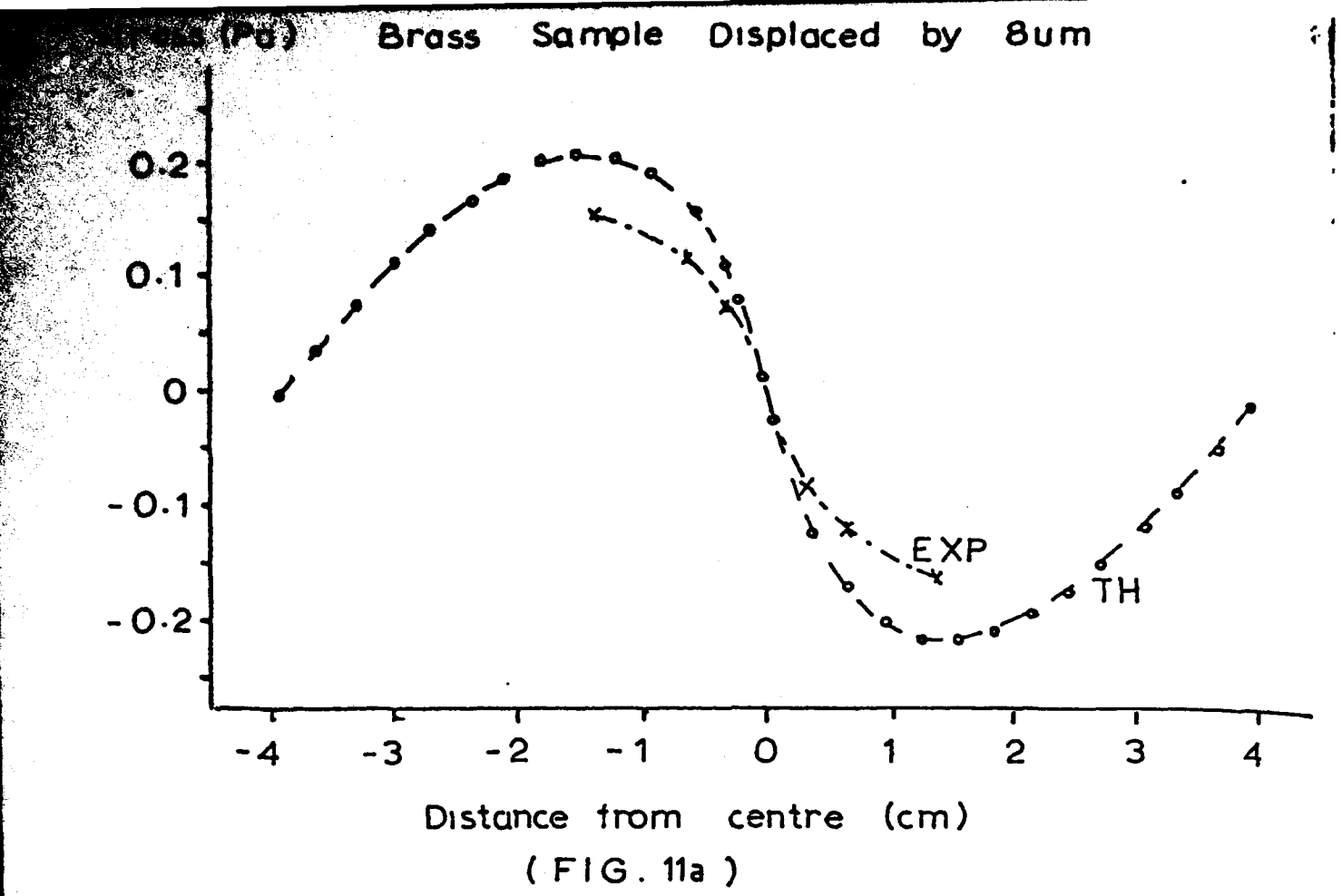

(FIG. 11a)

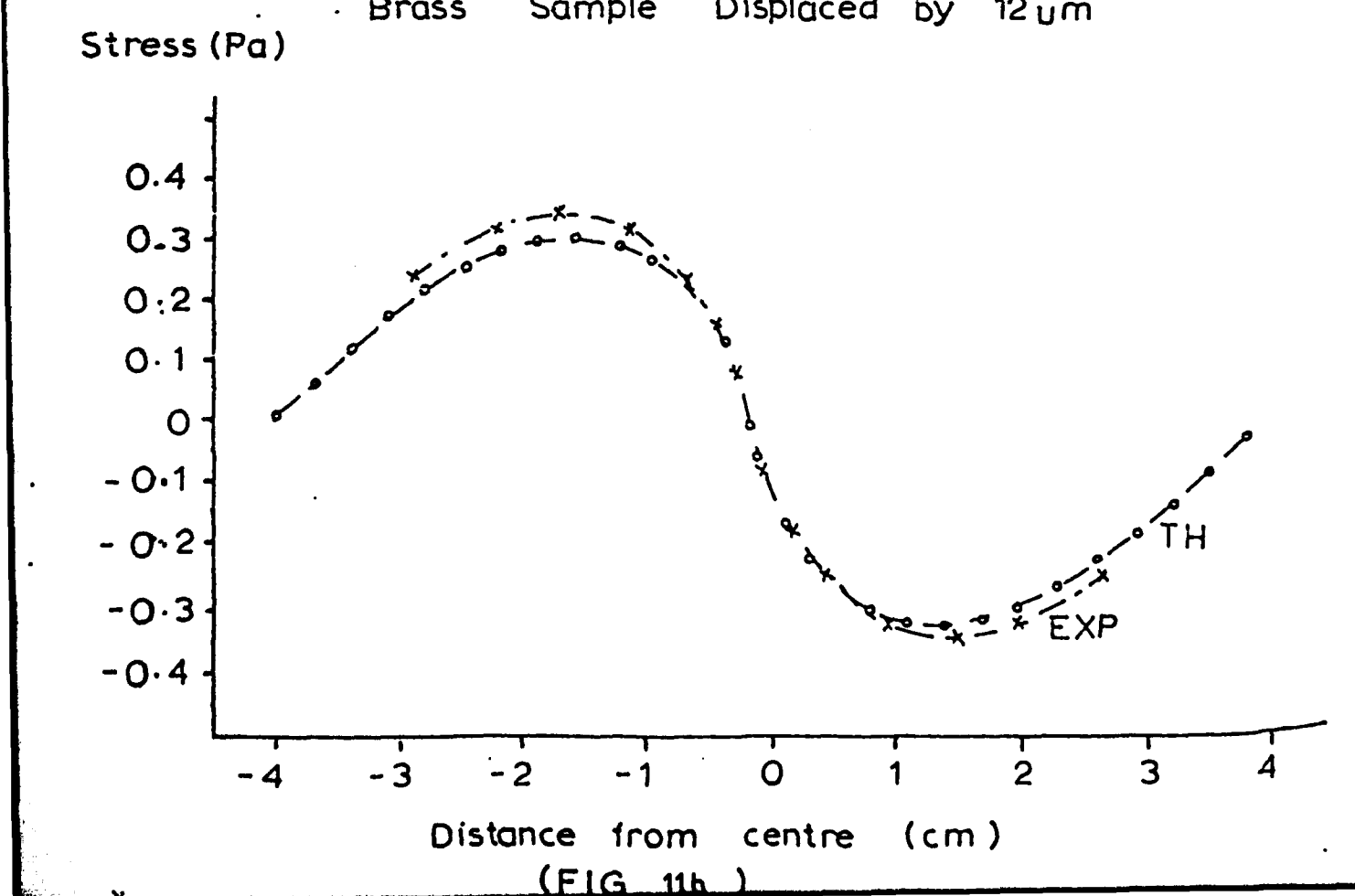

(FIG. 11b)

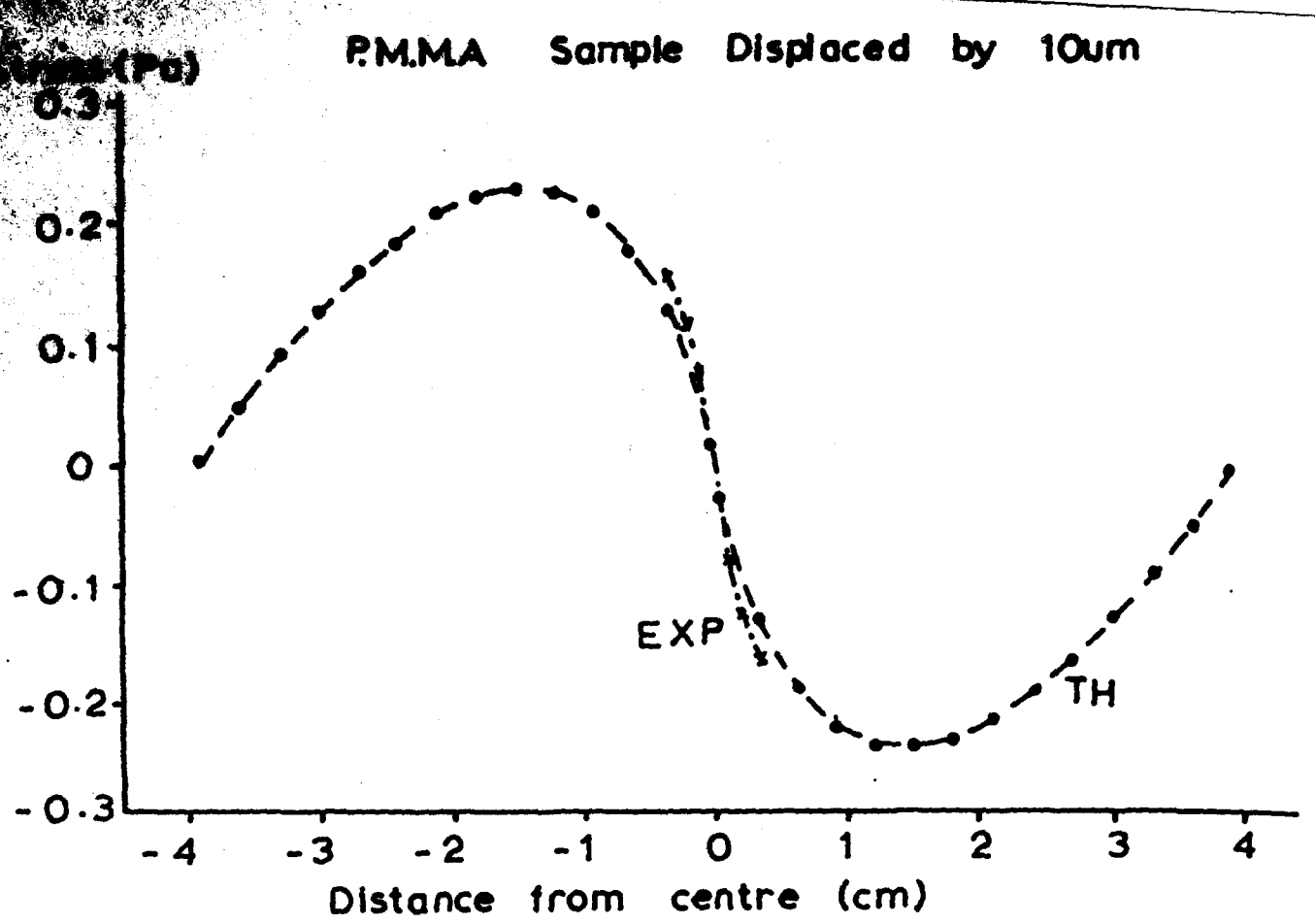

(FIG. 12a)

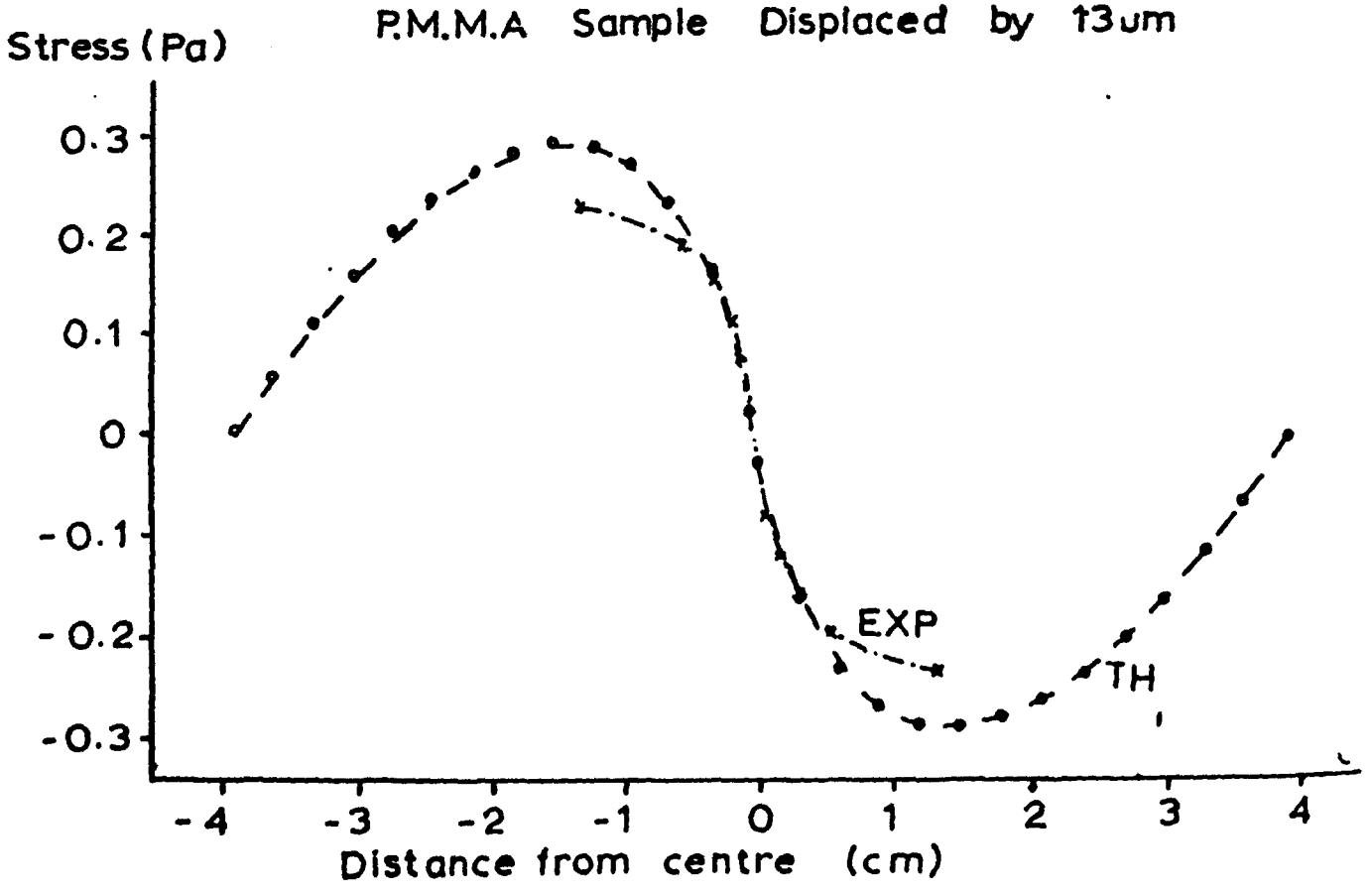

(FIG. 12b)

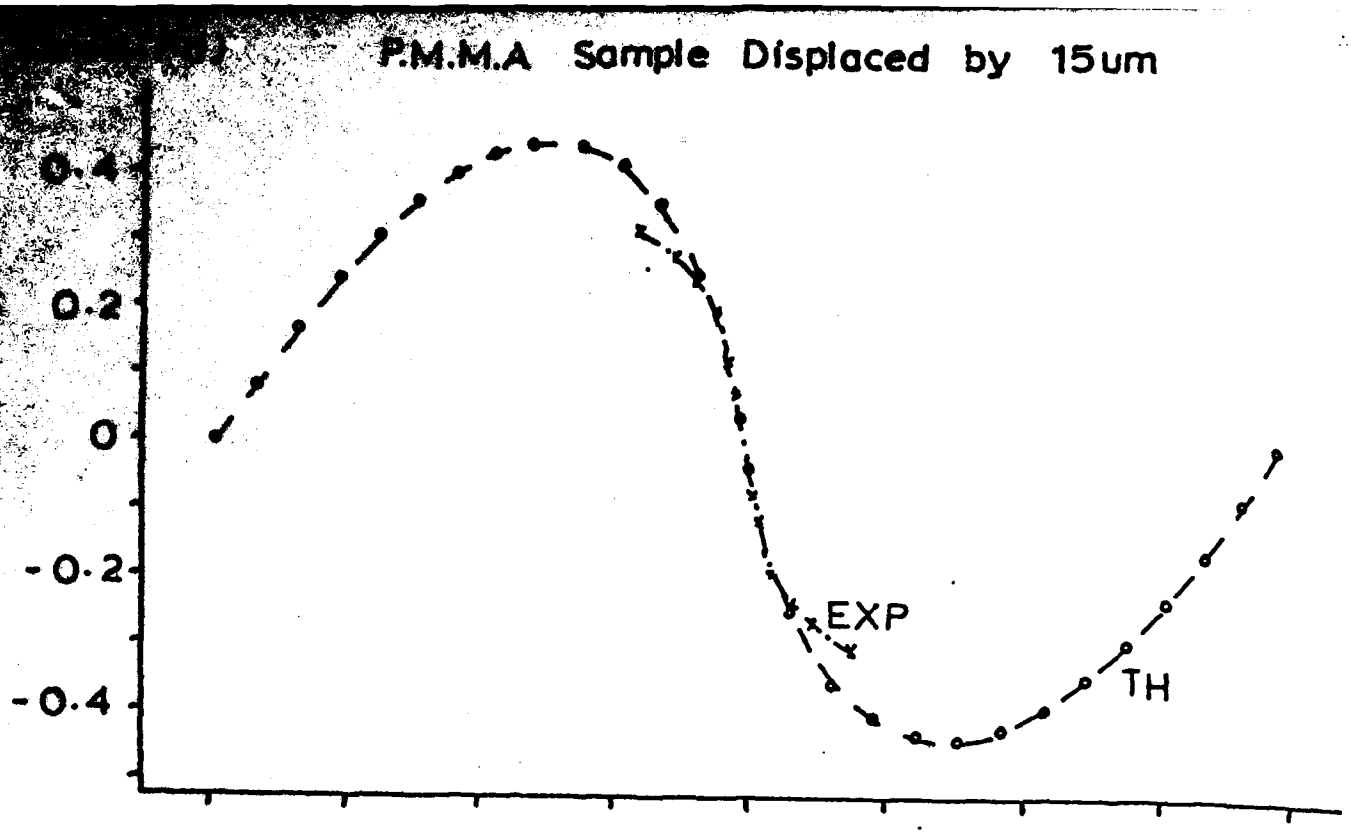

Distance from centre (cm)

(FIG. 12c:)

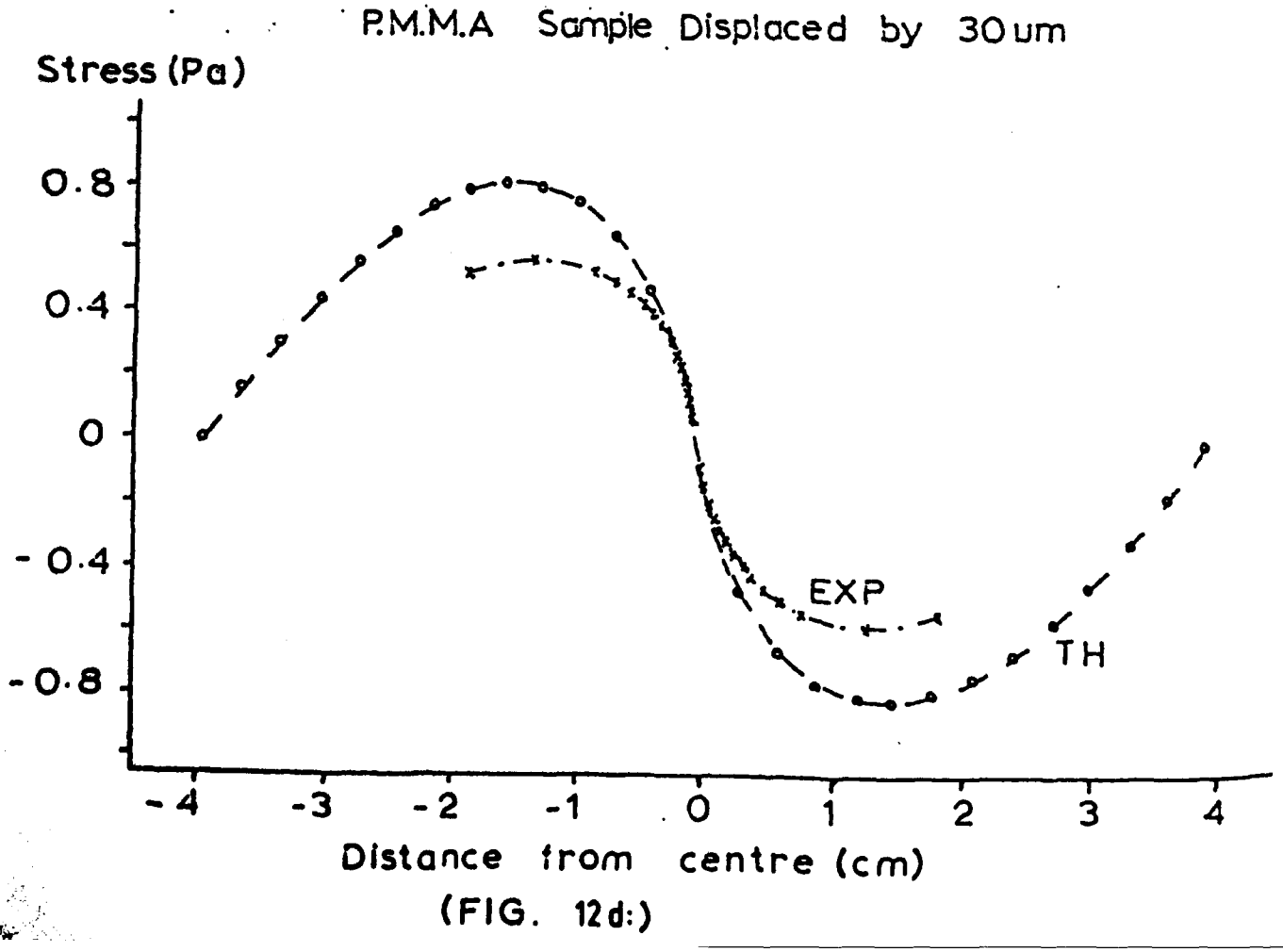

Distance from centre (cm)

(FIG. 12d:)

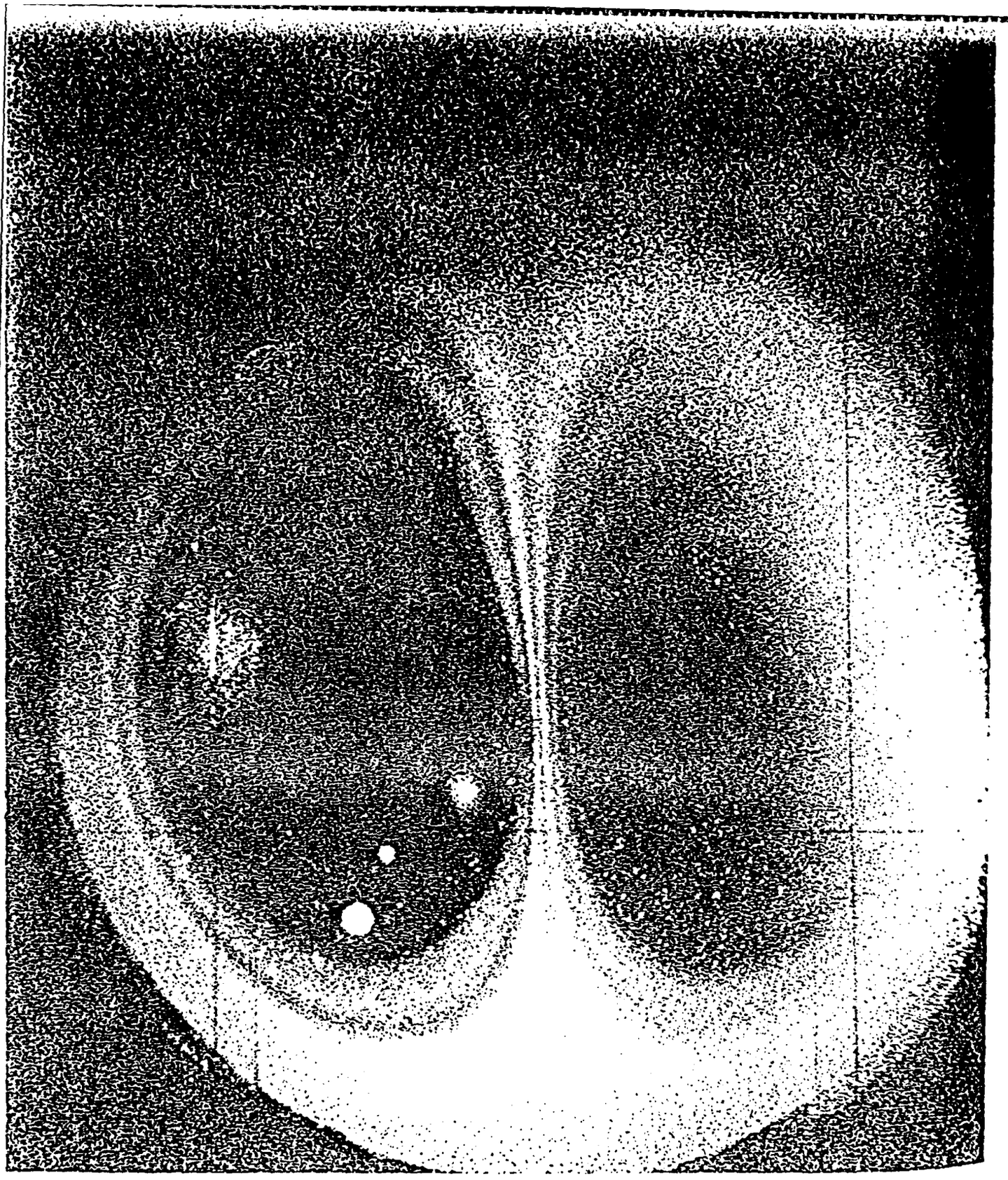

FIG. 13: 30s Prestress using 18 W Point Source Followed by 90 s of Further Heating

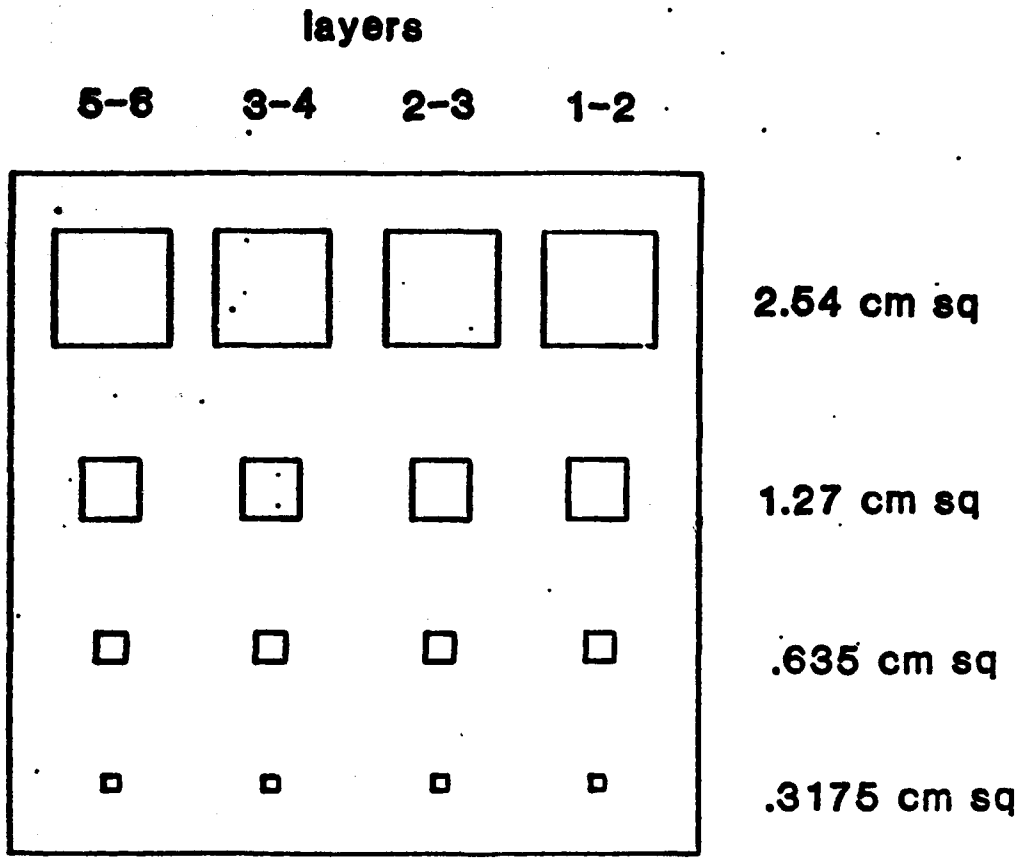

FIGURE 14: 10-PLY GRAPHITE EPOXY LAMINATE WITH EMBEDDED FLAWS

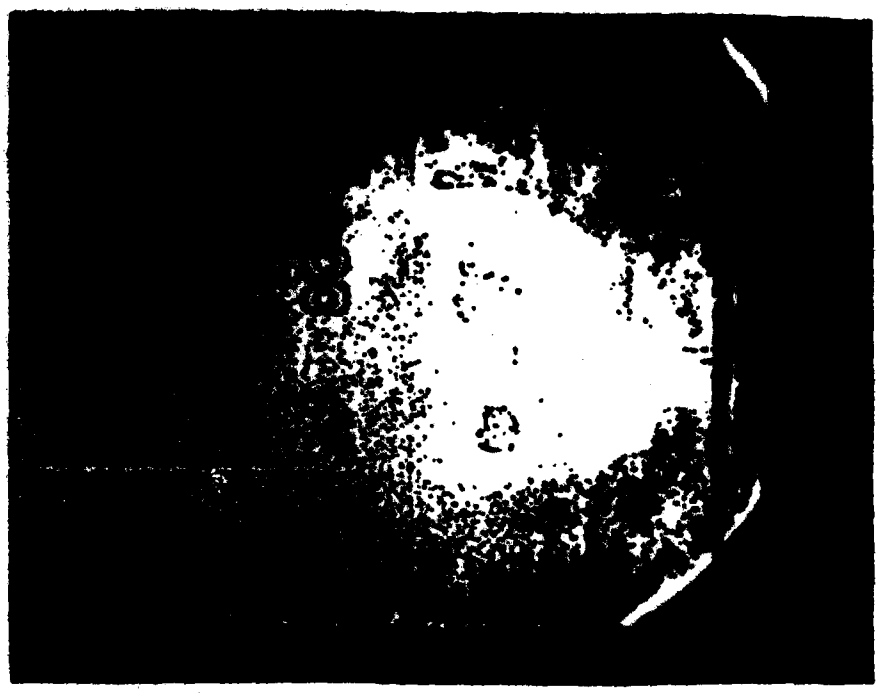

PULSED RUBY LASER ILLUMINATION SOURCE

Figure 15: Shearographic Delamination Detectio in Graphite Epoxy Laminate With Embedded Flaws

FIG. 16: "On-Line" Shearographic System using Electronic Processing

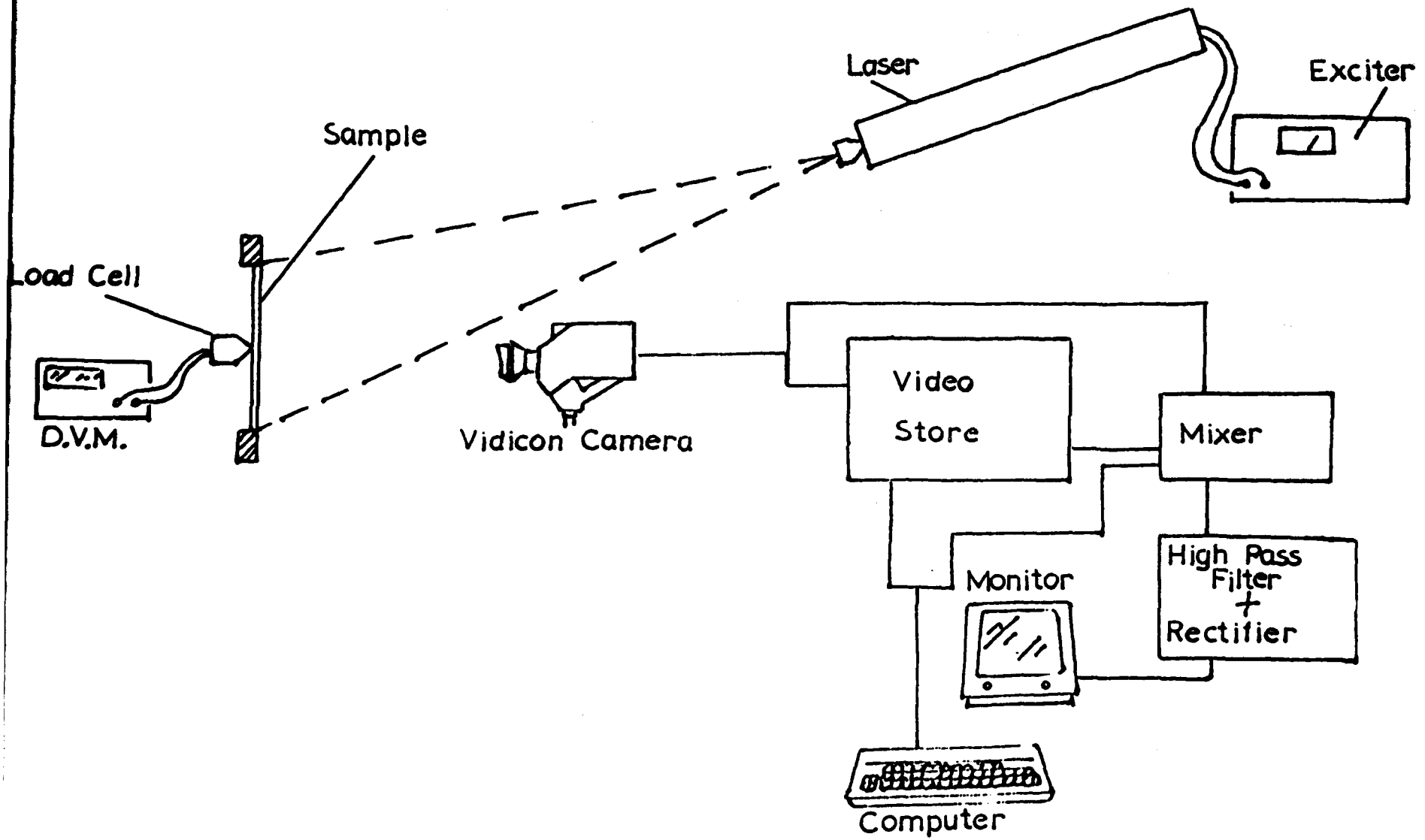

END

7-87

DTIC